Journal Pre-proof

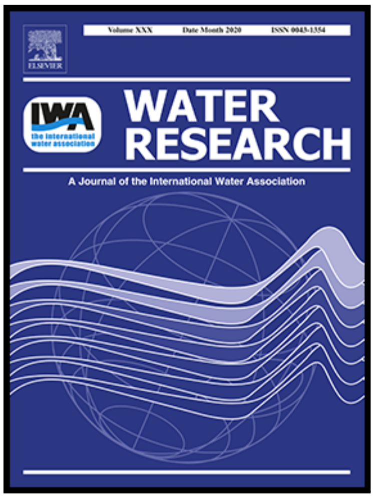

WaterROUTE: a model for cost optimization of industrial water supply networks when using water resources with varying salinity

Joeri Willet , Koen Wetser , Jouke E. Dykstra ,
Alessio Belmondo Bianchi , Gualbert Oude Essink ,
Huub H.M. Rijnaarts

PII: S0043-1354(21)00588-1
DOI: https://doi.org/10.1016/j.watres.2021.117390
Reference: WR 117390

To appear in: *Water Research*

Received date: 3 March 2021
Revised date: 22 June 2021
Accepted date: 23 June 2021

Please cite this article as: Joeri Willet , Koen Wetser , Jouke E. Dykstra , Alessio Belmondo Bianchi , Gualbert Oude Essink , Huub H.M. Rijnaarts , WaterROUTE: a model for cost optimization of industrial water supply networks when using water resources with varying salinity, *Water Research* (2021), doi: https://doi.org/10.1016/j.watres.2021.117390

WaterROUTE: a model for cost optimization of industrial water supply networks when using water resources with varying salinity

Joeri Willet [1] (corresponding author)

[1] Environmental Technology

Wageningen University

Bornse Weilanden 9, 6708 WG,

Wageningen

The Netherlands

Joeri.willet@wur.nl

Koen Wetser [1, 2]

[1] Environmental Technology

Wageningen University

Bornse Weilanden 9, 6708 WG,

Wageningen

The Netherlands

Koen.wetser@wur.nl

[2] Water and Food

Wageningen Environmental Research

P.O. Box 47

6700 AA Wageningen

the Netherlands

Jouke E. Dykstra [1]

[1]Environmental Technology

Wageningen University

Bornse Weilanden 9, 6708 WG,

Wageningen

The Netherlands

jouke.dykstra@wur.nl

Alessio Belmondo Bianchi[1]

[1]Environmental Technology

Wageningen University

Bornse Weilanden 9, 6708 WG,

Wageningen

The Netherlands

alessio.belmondobianchidilavagna@wur.nl

Gualbert Oude Essink [2, 3]

[2] Department of Physical Geography,

Utrecht University

Utrecht

Netherlands

Gualbert.OudeEssink@deltares.nl

[3] Unit Subsurface and Groundwater Systems,

Deltares

Utrecht

Netherlands

Huub H. M. Rijnaarts [1]

[1]Environmental Technology

Wageningen University

Bornse Weilanden 9, 6708 WG,

Wageningen

The Netherlands

huub.rijnaarts@wur.nl

Declarations of interest: none

Graphical_Abstract

Highlights

Using regional brackish water resources to create regional water supply networks

- Variations in groundwater salinity over time were modeled at a high spatial resolution
- The lowest cost Water Supply Network is determined while mixing of water with different salinities is considered
- Small variations in demand salinity cause large differences in the optimal network costs
- The WaterROUTE model links groundwater modelling with long term water supply planning

Abstract

Water users can reduce their impact on scarce freshwater resources by using more abundant regional brackish or saline groundwater resources. Decentralized water supply networks (WSN) can connect these regional groundwater resources with water users. Here, we present WaterROUTE (Water Route Optimization Utility Tool & Evaluation), a model which optimizes water supply network configurations based on infrastructure investment costs while considering the water quality (salinity) requirements of the user. We present an example simulation in which we determine the optimal WSN for different values of the maximum allowed salinity at the demand location while supplying 2.5 million m^3 $year^{-1}$ with regional groundwater. The example simulation is based on data from Zeeuws-Vlaanderen, the Netherlands. The optimal WSN configurations for the years 2030, 2045 and 2110 are generated based on the simulated salinity of the regional groundwater resources. The simulation results show that small changes in the maximum salinity at the demand location have significant effects on the WSN configuration and therefore on regional planning. For the example simulation, the WSN costs can differ by up to 68% based on the required salinity at the demand site. WaterROUTE can be used to design water supply networks which incorporate alternative water supply sources such as local brackish groundwater (this study), effluent, or rainwater.

Keywords: industrial water use, water supply network, network optimization, regional planning, alternative water sources, groundwater, salinity

1 Introduction

Global water consumption has increased more than fivefold in the 20th century and is expected to keep growing in the 21st century (Gleick, 2003; Shiklomanov, 1998). The combination of population growth (United Nations et al., 2019; Vörösmarty et al., 2000), overextraction (UN Water - FAO, 2007), contamination (UNEP, 2016), and hydrological changes due to climate change (Bates et al., 2008; Vörösmarty et al., 2000) will threaten water security around the world. Water scarcity is projected to increase (Hanasaki et al., 2013) and is increasingly considered a systemic risk to human welfare and biodiversity (Mekonnen and Hoekstra, 2016). New concepts for human water supply are needed to alleviate water scarcity for humanity and nature.

Industrial activities constitute a small fraction of the global water footprint (4.4%) (Hoekstra and Mekonnen, 2012) but have a high local water use intensity. Industrial facilities are generally located close to an abundant water source or large quantities of water are transported towards the industrial site to cover the demand. Historically, industries rely on centralized water supply infrastructures to transport water (Domènech, 2011; Gleick, 2003). The use of alternative local water resources can reduce the environmental impact of industrial water supply and requires a transition to decentralized water supply systems. Decentralized systems can alleviate environmental impacts while also reducing costs (investment, operational, network maintenance) and provide greater supply security (Domènech, 2011; Leflaive, 2009; Piratla and Goverdhanam, 2015). Decentralized systems can provide water from local surface water and groundwater sources such as local fresh water, rainwater, treated wastewater effluents, and brackish water (the focus of this study). The use of several supply sources creates the possibility for delivering water -after mixing- at the desired quality (Leflaive, 2009) and can lower costs by using local water supply sources to reduce total transport distance. This study focuses on delivering the desired quality when mixing groundwater with different salinities.

Optimizing the layout of a water supply network (WSN) is needed to minimize the high investment costs for piping infrastructure (Plappally and Lienhard, 2013). The costs for placing piping infrastructure depend on sub-soil characteristics, the land use where pipelines are to be placed, local policies, and property rights (Chee et al., 2018). Considering the differences in local pipeline construction costs at a high spatial resolution can significantly reduce overall capital investment costs (Feldman et al., 1995; Zhou et al., 2019).

The great number of potential pipeline connections in decentralized systems requires model-based approaches to generate cost effective designs. Model-based approaches are extensively used in the area of Integrated Water Resources Management (IWRM) (Medema et al., 2008). The system level analysis of IWRM is valuable for regional scale planning since it evaluates economic, environmental and social benefits simultaneously (Haasnoot et al., 2012; Savenije and van der Zaag, 2008). For an overview of the licensed and open source models available to decision makers in IWRM see: Awe et al., 2019; Clark and Cresswell, 2011; Sieber and Purkey, 2015; Sonaje and Joshi, 2015.

In this study we present WaterROUTE (Water Route Optimization Utility Tool & Evaluation), a model that adds new functionality to the previously developed WSN model (Willet et al., 2020). The original WSN model generates regional water supply networks only based on water quantity requirements. In the work presented here, the previously developed WSN model is extended to include water quality, specifically in terms of salinity. The addition of water quality as a design criterion for water supply networks is crucial to design regional decentralized water supply networks. The inclusion of water quality makes the delivery of water at the desired quality possible by mixing. In this study WaterROUTE is used to demonstrate how brackish/saline groundwater resources, exploited at sustainable yields, can serve as potential alternative water resources for industrial use. Brackish water resources can ensure a sustainable water supply when combined with optimal network layouts and desalination (Caldera and Breyer, 2017; Reddy and Ghaffour, 2007). For the first time, to our knowledge, we present and apply a modeling approach to create water supply network layouts with optimal pipeline routing at a high spatial resolution, connecting supply sources with different salinities, which also accounts for pipeline placement costs.

WaterROUTE optimizes water supply network configurations according to site-specific demands for water quality and quantity with water supply sources that have different and variable water qualities. With this functionality we connect regional hydrological modeling with planning of water supply infrastructure. The model generates the optimal network configuration and quantity of water needed from each supply source to satisfy the (industrial) demand without trespassing sustainable limits for water extractions. WaterROUTE is a valuable tool for IWRM and regional planning in areas where maximum sustainable yields of aquifers need to be enforced. Areas of particular interest are freshwater scarce areas with intensive industrial activities for which lower quality water can be used and where alternative (ground)water resources are available. We present and example simulation with regional brackish groundwater resources as the alternative water source for an industrial site.

2 Methodology

WaterROUTE is an optimization and visualization model which calculates optimal water supply network configurations. The optimization model mixes water streams with different qualities to supply a single demand location with a desired water quality. Mixing of water is a new and essential functionality to design decentralized water supply networks that use alternative water resources with different qualities.

In WaterROUTE, water supply and demand sites are represented as vertices and pipeline connections are represented as edges. The vertex and edge representation of (water) transport networks is commonly used for optimization (Mala-Jetmarova et al., 2017) and was previously used for network design without mixing in Willet et al. (2020).

WaterROUTE requires two inputs: the available water sources in a region and a preliminary network from which the optimal network configuration is selected. The preliminary network is created by determining the lowest cost routes between demand and supply locations using geographic information systems (GIS) methods. The inputs are processed by the WaterROUTE optimization model to yield the network configuration with the lowest cost for a specific water demand at the demand location (Section 2.1 - 2.6). The outputs are then visualized with GIS software for evaluation and decision making. An overall representation of WaterROUTE[1] is shown in Figure 1.

[1]Software used for the input data: MODFLOW (version: MODFLOW-96), MOC3D (version: 1.1 05/14/9), MOCDENS3D (adaptation to MOC3D as described in [Oude Essink (2001); Oude Essink et al. (2010)]
Software used for the preliminary network layout and visualization: ArcGIS Pro (build number: 2.4.19948)
Software used for the optimization: Python (version: 3.7.9), Gurobi (version: 9.0.3).

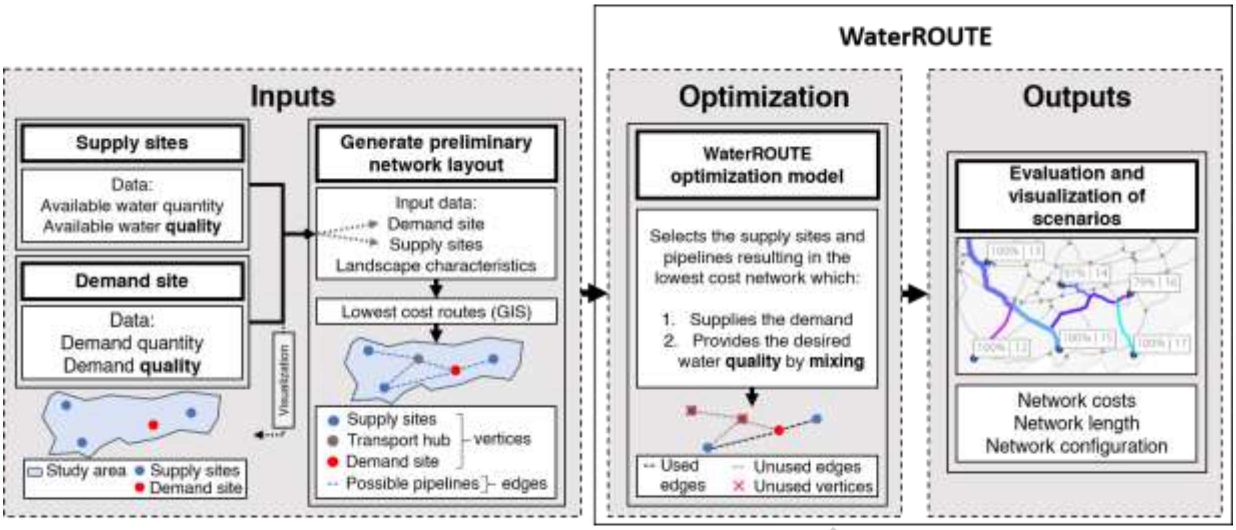

Figure 1 The model framework of WaterROUTE

2.1 Formulation and parameters

The WaterROUTE optimization model is a variation of the fixed charge network flow problem (FCNFP) (Hirsch and Dantzig, 1968; Kim and Hooker, 2002). In this study, we alter the original FCNFP formulation to include water quality parameters as a constraint. The water quality parameter included in this study is the salinity (the chloride concentration) of groundwater. Water may mix throughout the network, yet the water reaching the demand location must not exceed the maximum salinity defined by the user.

The WaterROUTE optimization problem is described as a planar mathematical system represented by vertices (V_i) and edges (E_{V_i,V_j}). Vertices represent supply locations, demand locations, and transport hubs/junctions. Edges represent the possible pipeline connections between vertices. Each vertex (V_i) has a chloride concentration (c_i) and an associated water supply or demand (s_i). Three situations can be distinguished for each vertex:

- when $s_i > 0$, vertex V_i is a water source, s_i is the volume of water available, and c_i is the chloride concentration of the available water;
- when $s_i < 0$, vertex V_i is a demand location, s_i is the volume of water to be supplied, and c_i is the maximum chloride concentration for the water;
- when $s_i = 0$, vertex V_i is a transport hub/junction in the network where water can mix.

Edges (E_{V_i,V_j}) transport water from vertex V_i into vertex V_j. Each edge (E_{V_i,V_j}) has two variables: flow of water ($x_{i,j}$) and flow of product ($p_{i,j}$), the product is the amount of chloride (in mgCl$^-$ day^{-1}). The total product is determined based on the concentration and amount of water extracted from each supply vertex. Each edge has an associated cost per unit flow per km ($r_{i,j}$), and a length in km ($l_{i,j}$). Additional parameters are the maximum flow ($u_{i,j}$) and maximum product capacity ($t_{i,j}$) over each edge. We define a maximum allowed concentration (c_m) that is used to constrain the final quality of the supplied water. Table 1 gives an overview of the parameters in the WaterROUTE optimization problem formulation.

Table 1 Overview of parameters used to formulate the optimization problem with mixing and quality constraints.

Parameter	*Description*
V_i	Vertex i represents the source or demand location i
$E_{i,j}$	Edge i,j represents the pipeline connection between vertex i (V_i) and vertex j (V_j)
s_i	Water supply ($s_i > 0$) or demand ($s_i < 0$) at vertex i (m^3 day^{-1})
c_m	Maximum allowed concentration at the demand location ($mgCl^-$ L^{-1})
c_i	Product concentration at vertex i if $s_i > 0$ or target concentration $c_i \leq c_m$ if $s_i < 0$ at vertex i ($mgCl^-$ L^{-1})
$x_{i,j}$	Flow of water through edge i,j (decision variable in the optimization problem) (m^3 day^{-1})
$p_{i,j}$	Flow of product (chloride) through edge i,j ($mgCl^-$ day^{-1})
$u_{i,j}$	Maximum flow capacity of pipeline section (edge) i,j (m^3 day^{-1})
$t_{i,j}$	The maximum allowed product concentration for water flowing through pipeline i,j ($mgCl^-$ L^{-1})
$r_{i,j}$	Pipeline investment costs per meter (€ m^{-1}) per unit flow (m^3 day^{-1}) → (€ m^{-1} / m^3 day^{-1}) (based on a maximum flow velocity of 1.5 m s^{-1})
$l_{i,j}$	The length of the pipeline represented by edge i,j

2.2 Objective function

The WaterROUTE optimization problem minimizes the total investment costs for pipeline placement (TPPC, Total Pipeline Placement Costs). The TPPC is the sum of the costs of the individual pipeline segments required for the complete water supply network. Due to the limited number of available pipeline diameters the pipeline investment costs (r_{ij}) increase with steps depending on the flow required. The interaction between the available pipeline diameters, flow requirements, and flow velocity leads to investment costs which increase with a stepwise pattern (see Supplementary Information 1). A stepwise increase in costs is referred to as a stairwise arc cost function (Bornstein and Rust, 1988; Du and Pardalos, 1993; Holmberg, 1994). In this study, pipeline diameters with increments of 100 mm and a maximum flow velocity of 1.5 m s^{-1} are used. The steps in the cost function were determined for a flow range between 0 and 5.5 Mm^3 $year^{-1}$ by increasing the flow with steps of 0.1 Mm^3 $year^{-1}$ with a peak factor of 1.5 (Supplementary Information 1). The stepwise behavior is incorporated in the objective

$$TPPC = \sum_{(i,j)\in E} f_{ij}(x_{ij}) \tag{1}$$

function, given by

$$f_{ij}(x_{ij}) = \begin{cases} 0 & x_{ij} = 0, \\ r_{ij}^{k} l_{ij} & \lambda_{ij}^{k-1} < x_{ij} \leq \lambda_{ij}^{k} \end{cases} \quad \text{with } r_{ij}^{k} \text{ and } \lambda_{ij}^{k} \text{ as defined in Table 2} \tag{2}$$

The stepwise costs for placement of new pipelines $f_{ij}(x_{ij})$ are defined by

where x_{ij} is the flow, and λ_{ij}^{k} represent the breakpoints in the cost function based on the flow in the pipeline. When there is no flow over an edge ($x_{ij} = 0$) no investment costs are incurred (resulting in $f_{ij}(x_{ij}) = 0$) and the edge is considered unused. The possible pipeline diameters are represented with an index $k = 1$ to $k = 5$. The length of the pipeline segment is l_{ij}, and r_{ij}^{k} are the investment costs per meter (Table 2).

Table 2 Pipeline investment costs for a flow between 0 and 5.5 million m^3 year^{-1} (0 – 15068 m^3 day^{-1}) based on design guidelines for water distribution networks (Mesman and Meerkerk, 2009). Investment costs were determined in consultation with experts in the field of water distribution in the Netherlands.

k	λ_{ij}^{k}	**FLOW OVER EDGE x_{ij} (m^3 day^{-1})**	***PIPELINE DIAMETER (mm)***	***INVESTMENT COSTS r_{ij}^{k} (€ m^{-1})***

	0	0	*0*	*0*
1	*548*	$0 < x_{ij} \leq 548$	*100*	*50*
2	2466	$548 < x_{ij} \leq 2466$	*200*	*100*
3	5753	$2466 < x_{ij} \leq 5753$	*300*	*150*
4	9863	$5753 < x_{ij} \leq 9863$	*400*	*200*
5	15068	$9863 < x_{ij} \leq 15068$	*500*	*250*

2.3 Constraints: water quantity and pipeline capacity

The amount of water extracted from any vertex should be smaller than or equal to the total amount of

$$\sum_{(i,j)\in E} x_{ij} - \sum_{(j,i)\in E} x_{ji} \leq s_i \qquad \forall i \in V \qquad (3)$$

water available at that vertex, and is ensured by

which ensures the water balance at each vertex. We apply this constraint to every vertex i in the set of vertices V.

Edges can be assigned a flow of 0, meaning the edge is not used, but the flow should not exceed the

$$0 \leq x_{ij} \leq u_{ij} \qquad \forall (i,j) \in E \qquad (4)$$

maximum capacity (u_{ij}) of the edge, which is ensured by

which represents the allowed minimum and maximum flow over each edge. The maximum capacity over the edges in the preliminary network is equal to the demand volume of the demand site because existing pipelines are not included in the example simulation. If existing pipelines are re-used the maximum capacity over an edge depends on the size of the existing pipeline section. We apply the constraint to every edge.

The sum of the water flows exiting a vertex should be equal to the sum of the water flows entering the

$$\sum_{(i,j)\in E} x_{ij} - \sum_{(j,i)\in E} x_{ji} = 0 \qquad \forall i \in V; s_i = 0 \quad (5)$$

vertex if the vertex is a transport hub ($s_i = 0$)

which ensures that the outgoing flow (x_{ij}) is equal to the incoming flow (x_{ji}) for all transport hubs ($s_i = 0$).

Supply sites located in the middle of the network can perform a dual function: providing water to the network while also serving as a transport hub (see Figure 2).

Figure 2 Dual function of a supply site: supply location and transport hub. The outgoing flow must be larger or equal to the incoming flow.

The water flowing out from any supply vertex needs to be larger or equal to the water flowing towards

$$\sum_{(i,j)\in E} x_{ij} - \sum_{(j,i)\in E} x_{ji} \geq 0 \qquad \forall i \in V; s_i > 0 \quad (6)$$

the supply vertex and is ensured by

The sum of the water flows out (x_{ij}) from a supply site vertex ($s_i > 0$) must be greater than or equal to the sum of the water flows entering (x_{ji}) the vertex.

2.4 Constraints: water quality

WaterROUTE generates network layouts that supply water with a specific maximum concentration at the demand site. For mixing of water flows up to a maximum concentration we formulate the constraints in Eq. (7) - (11). These constraints control the amount of product (p_{ji}) flowing over an edge ($E_{i,j}$).

The amount of product (mass) extracted from a supply vertex must be equal to the amount of water (volume) extracted from that vertex times the concentration (mass/volume) at that vertex if the vertex

$$\sum_{(i,j)\in E} p_{ij} - \sum_{(j,i)\in E} p_{ji} = \left(\sum_{(i,j)\in E} x_{ij} - \sum_{(i,j)\in E} x_{ji} \right) c_i \qquad \forall i \in V; s_i > 0 \qquad (7)$$

is a source ($s_i > 0$). We ensure this with

The constraint in Eq. (7) ensures that the water extracted from a supply vertex ($\sum x_{ij} - \sum x_{ji}$) times the concentration at the vertex (c_i) is equal to the product extracted ($\sum p_{ij} - \sum p_{ji}$).

The amount of product extracted from any supply vertex must be lower than or equal to the amount of

$$\sum_{(i,j)\in E} p_{ij} - \sum_{(j,i)\in E} p_{ji} \leq s_i \cdot c_i \qquad \forall i \in V;\ s_i > 0 \qquad (8)$$

product extractable from that vertex

The product available at a supply vertex is determined by multiplying the concentration at the vertex by the amount of water available ($s_i \cdot c_i$)

Similar to the water flows for a supply site functioning as a transport hub, the sum of the product flows towards the vertex must be lower than or equal to the sum of the product flows exiting the vertex. This

$$\sum_{(i,j)\in E} p_{ij} - \sum_{(j,i)\in E} p_{ji} \geq 0 \qquad \forall i \in V;\ s_i > 0 \qquad (9)$$

is achieved with

where $\sum p_{ij}$ is the outgoing product flow and $\sum p_{ji}$ is the incoming product flow.

The product flow (mgCl$^-$ day^{-1}) towards the demand site ($s_i < 0$) divided by the water volume (m^3 day^{-1}) towards the demand vertex must be lower or equal to the maximum allowed concentration. We ensure this with

$$\sum_{(i,j)\in E} p_{ij} - \sum_{(j,i)\in E} p_{ji} \geq \left(\sum_{(i,j)\in E} x_{ij} - \sum_{(i,j)\in E} x_{ji} \right) c_i \qquad \forall i \in V;\ s_i < 0 \qquad (10)$$

which is similar to Eq. (7), but the equality condition is replaced by an inequality condition and Eq. (7) is only applied to the demand location ($s_i < 0$). If an exact target concentration is required, the inequality condition in Eq. (10) is replaced by an equality condition.

If an edge is used the product flow should be larger than zero and the product flow must not exceed the

$$0 < p_{ij} \leq t_{ij} \cdot x_{ij} \qquad \forall (i,j) \in E \qquad (11)$$

maximum allowed concentration for water in the pipeline (t_{ij})

which can be used for the expansion of existing networks where the product concentration needs to be limited for certain pipelines.

2.5 Formulation overview and outputs

minimize	Objective function: TPPC of Equation (1)
subject to	Flow conservation: constraints (3), (5), (6)
	Physical bounds: constraints (4), (11)
	Product conservation: constraints (7), (8), (9), (10).

The complete formulation for the WaterROUTE optimization problem is written as

Solving the optimization problem yields the lowest cost WSN that supplies water with a concentration lower than or equal to the maximum allowed concentration at the demand location. The output of the problem is the water flow ($x_{i,j}$) over each edge of the preliminary network layout. Edges that are assigned a flow of zero (see Eq. (2) and Table 2) are not in use and do not contribute to the TPPC.

2.6 Special case: minimum salinity network determination

When the desired water quality is set to the minimum salinity achievable for a certain demand (see Supplementary Information 3) the supply sources can be determined before the network configuration optimization. Supply sites are ordered by increasing salinity and the cumulative water availability and associated salinity are calculated. The set of clusters which can supply the demand at the minimum salinity is determined from the cumulative water and salinity list. Clusters not in the set are removed from the WaterROUTE optimization model inputs and the optimal network is determined by omitting the water quality constraints. This procedure reduces calculation time considerably for large networks.

3 WaterROUTE example simulation inputs

WaterROUTE is demonstrated by generating water supply networks to supply an industrial site (DOW Terneuzen, in Zeeuws-Vlaanderen, the Netherlands) with local groundwater. The WaterROUTE model is used to investigate the effect of varying the maximum chloride concentration ($mgCl^{-} L^{-1}$) reaching the industrial site on the optimal WSN layout. WaterROUTE is used to generate water supply networks for 2030, 2045 and 2110 to account for changes in groundwater salinity, and a static demand of 2.5 Mm^{3} $year^{-1}$. The inputs for the example simulation are the available local groundwater sources (Section 3.1) and the preliminary network layout between the demand and supply locations (Section 3.2)

3.1 Groundwater salinity and availability

The groundwater in the example simulation comes from several well clusters identified based on the fresh-salt groundwater interface as well as the transmissivity, which affects the possibility to extract water, of the groundwater system in the region (see Willet et al., 2020). The regional groundwater system has been extensively monitored, mapped and modelled in the past and shows the presence of fresh groundwater resources on top of groundwater with a higher salinity (Delsman et al., 2018).

A submodel of an existing, calibrated, 3D variable-density groundwater flow and coupled salt transport model is used to simulate changes in groundwater salinity and piezometric heads over time, for the period 2020-2110 (Van Baaren et al., 2016). The submodel covers Zeeuws-Vlaanderen, The Netherlands and has the dimensions 70 km west-east by 28 km north-south by 143 m thick. The 3D groundwater model uses the MODFLOW (Michael G. McDonald and Arlen W. Harbaugh, 1988) based computer code MOCDENS3D (Faneca Sànchez et al., 2012; Oude Essink et al., 2010). It uses 40 model layers (with grid cell thicknesses varying from 0.5 m to 10 m with increasing depth) to reproduce the movement of groundwater salinity in the vertical direction; resulting in over 7.8 million grid cells. Changes in groundwater salinity are simulated by advection and hydrodynamic dispersion. Complex geology (horizontal and vertical hydraulic conductivities) (Stafleu et al., 2011) and the mapped groundwater salinity (via intensive airborne electromagnetics (Delsman et al., 2018)) are inserted in the model. Stresses to the groundwater system consist of seasonal natural groundwater recharge (from de Lange et al., 2014), six surface water types (sea and estuarine waters, lakes, canals, (small) rivers, watercourses up to ditches), a shallow drainage system, and groundwater extraction wells (retrieved from a database of the Water Board Scheldestromen). The surface water and drainage systems are inserted into the model using an accurate Digital Elevation Model (Actuel Hoogtebestand Nederland, 2020) (resolution 5*5 m). Boundary conditions (the sea, the estuary, and the Belgian hinterland) complete the existing 3D groundwater model (Van Baaren et al., 2016).

The original 3D variable-density groundwater flow and coupled salt transport model has been calibrated based on a database of piezometric heads (calibration was done in Van Baaren et al., 2016). The model has been published in a Deltares report (Van Baaren et al., 2016). The final calibration set of piezometric heads consisted of 606 observations for the entire area of the province of Zeeland from the database of dinoloket.nl, over the period 1-1-1991 up to 31-12-2000. The effect of the groundwater density in the observation wells on the heads was considered (Post et al., 2007). We used the code PEST, the most widely used calibration software for groundwater in the world (Doherty, 2005). Parameters that have been changed during the calibration are the horizontal hydraulic conductivity of the aquifers, the vertical hydraulic conductivity of the aquitard, the hydraulic resistance from/to the surface water system and finally the groundwater recharge. The results for Zeeuws-Vlaanderen are as follows: the median of the difference between the calculated minus the measured heads changes from 0.18 m to -0.009 and the average absolute difference between the calculated minus the measured heads changes from 0.29 m to 0.24 m. We believe these differences are good enough calibration results. Validation of the model has not been performed as the entire dataset was believed to be needed for the calibration.

In this study, the 3D groundwater model simulates the effect of multiple brackish groundwater extractions (used as the alternative water supply source) over the well clusters on the groundwater salinity over time and the piezometric heads in the vicinity of well clusters. In Willet et al. (2020), analytical equations were used to estimate the upconing of the interface between fresh and saline groundwater (Dagan and Bear, 1968) and the drawdown of the phreatic groundwater level (Bruggeman, 1999). The numerical 3D groundwater model incorporates hydro(geo)logical details of the local setting (the heterogeneous salinity distribution, interaction with the surface water system, geology), includes changes in groundwater salinity due to extraction wells, and thus produces more accurate results than the previously used analytical methods. The same locations of the 2079 extraction wells in the 25 well clusters identified in Willet et al. (2020) were used. The number of extraction wells per well cluster varies, from a minimum of 10 to a maximum of 331. The extraction wells are positioned at least 100 m from each other to limit strong drawdown superposition. For further details on well placement and extraction rates see Supplementary Information 2.

The surface water boundary is modelled with a fixed salinity concentration and does not change over the entire simulation period. There is not enough surface water salinity data to insert a seasonal varying surface water salinity boundary condition (though the model can do so; a seasonal varying surface water head boundary was modeled). Several surface water features in the Zeeuws-Vlaanderen region are draining from the groundwater system or are not active in summer. The fresh groundwater recharge is likely a dominant source of fresh water that enters the wells, given that small water courses and ditches are the main surface water phenomena in this region.

To meet environmental targets (e.g. Natura2000) and to limit drought effects, the maximum drawdown of the phreatic groundwater level is set to 50 mm (Figure 3). The exact maximum allowed groundwater extraction rate per well was determined iteratively while meeting the maximum drawdown of the phreatic groundwater level. In the first iteration step, the starting groundwater extraction rates as used in Willet et al. (2020) are taken. Within ten iteration steps, the changes in groundwater extraction rates become negligible. The 3D groundwater model considers interferences in piezometric head and groundwater salinity over time of nearby extraction wells. The overall salinity of a well cluster is determined based on the sum of the salt (in mgCl$^-$ day^{-1}) extracted from all wells in the well cluster and the sum of the water (m^3 day^{-1}) extracted from all wells in the well cluster.

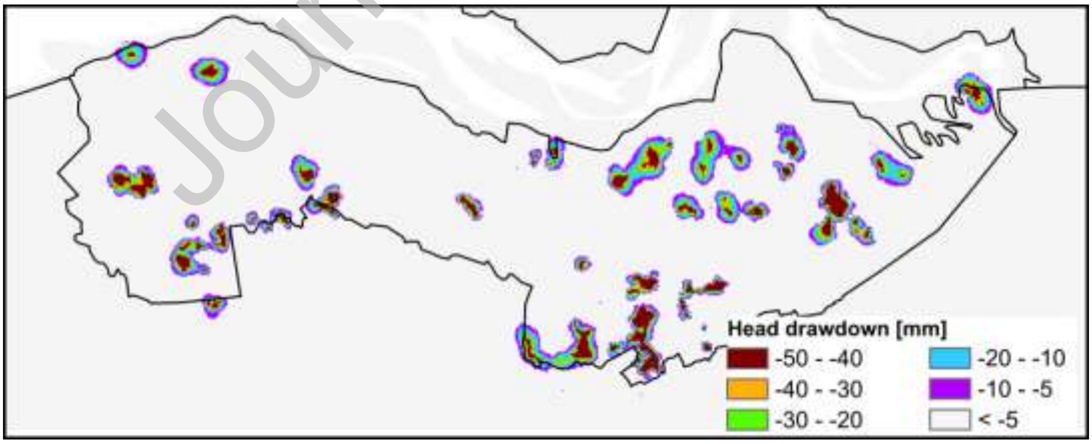

Figure 3 modelled drawdown of the piezometric head per well cluster, caused by 2079 extraction wells distributed over 25 well clusters. The maximum drawdown is 50 mm wherever extraction wells are positioned.

The available groundwater from all well clusters in the study area is 6.119 Mm^3 $year^{-1}$ while having a maximum drawdown of 50 mm. Changes in precipitation patterns and the associated effects on groundwater availability were not included. The overall combined salinity of all 2079 wells over 25 well clusters is 472 $mgCl^-$ L^{-1} in 2020. In 2020, there are two well clusters (in the north-west and center of the study area) which are significantly more saline (Figure 5). Operating all well clusters at the maximum extraction rate increases the salinity of most clusters. The average chloride concentration increases from 472 $mgCl^-$ L^{-1} in 2020 to 852 $mgCl^-$ L^{-1} in 2030, 981 $mgCl^-$ L^{-1} in 2045, and 1095 $mgCl^-$ L^{-1} in 2110 (see Supplementary Information 4 for details on water availability at each well cluster). When water extractions start, the salinity of well clusters changes quickly within (on average) 10 years but stabilizes over time when a new equilibrium in the subsoil is reached (see Supplementary Information 5). For some well clusters, a significant decrease in salinity (i.e. freshening), occurs because fresh water from the surface water system moves towards the extraction point when groundwater is extracted (clusters 10, 13, 16, and 19, see Figure 4). Well cluster 24 first becomes more saline between 2020 and 2030 and then becomes slightly fresher up to 2110. The salinization or freshening rate of well clusters is not uniform for all clusters, and therefore, the optimal WSN configuration with the lowest costs is specific for each period and demand quality.

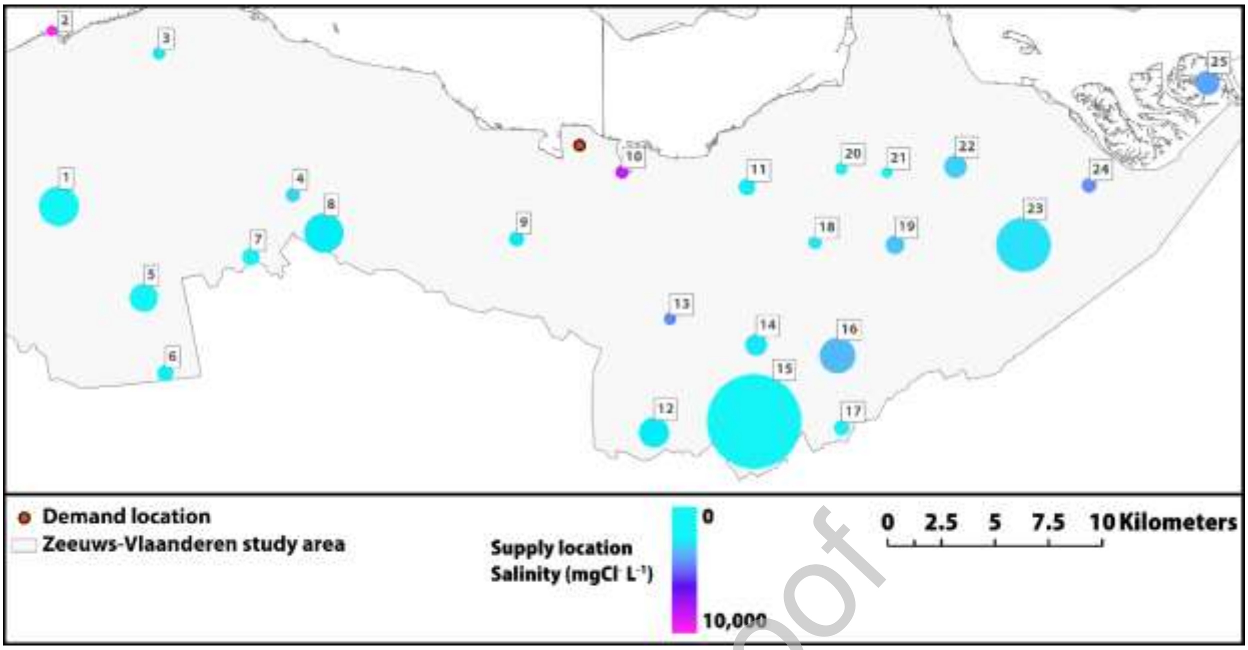

Figure 5 Modelled groundwater supply locations in Zeeuws-Vlaanderen and salinity in 2020. Labels represent the well cluster numbers. The diameter of the marker represents the amount of water available. Most water is available at well cluster 15 (1.43 Mm^3 $year^{-1}$), and the least at well cluster 2 (0.01 Mm^3 $year^{-1}$).

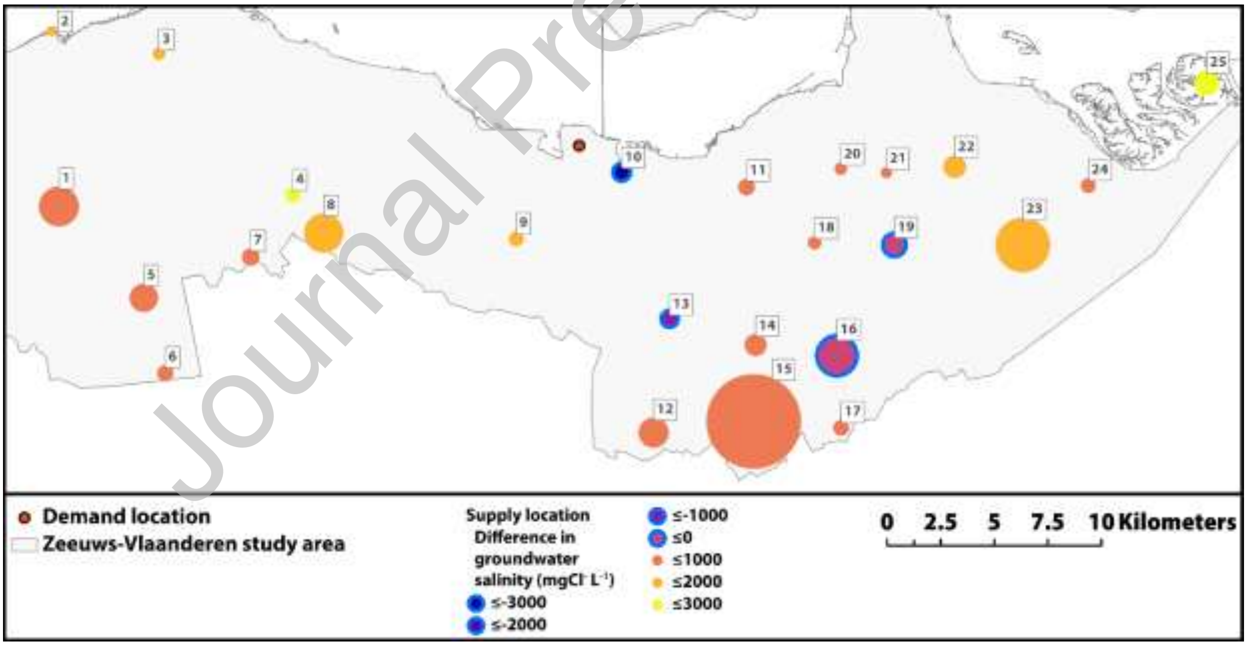

Figure 4 Modelled changes in groundwater salinity for well clusters in Zeeuws-Vlaanderen between 2020 and 2110 based on the extraction rates in Supplementary Information 4. These changes vary between -3412 $mgCl^- L^{-1}$ (water becoming fresher, well cluster 10) and 2785 $mgCl^- L^{-1}$ (water becoming more saline, well cluster 25). A blue outline indicates the well cluster becomes fresher. Labels represent the well cluster numbers. The diameter of the marker represents the amount of water available.

3.2 Preliminary network layout

The preliminary network layout is the complete set of possible pipelines connecting all the supply and demand locations in the study area. The WaterROUTE optimization model selects the subset of pipelines with the lowest total costs for a specific demand at the demand site. The selected subset is the optimal WSN configuration for a specific scenario. The preliminary network layout in this study represents a water supply network which still needs to be built but the same methodology can be applied for an existing (to be expanded) water supply network. The preliminary network for the Zeeuws-Vlaanderen region was generated following the steps as outlined in Willet et al. (2020), using lowest cost route methods with GIS software. The main steps to generate the preliminary network layout are:

(1) Creating a cost of passage surface based on local land-use types in collaboration with water supply experts (see Willet et al., 2020). A cost of passage surface is needed to include the local spatial data in the network optimization problem. Including local spatial data is important since the costs for placing pipeline infrastructure depend on the local land-use and subsurface characteristics (Feldman et al., 1995).

(2) Tracing the lowest cost route between each possible combination of supply and demand locations based on the cost of passage surface. The resulting network serves as the preliminary network layout for optimization. The use of lowest cost route methods is common for infrastructure routing (Atkinson et al., 2005; Collischonn and Pilar, 2000; Douglas, 1994).

The preliminary network has a total of 408 pipeline segments and 243 transport hubs to connect the 25 groundwater supply locations and the single demand location (see Supplementary Information 7).

4 Results

WaterROUTE is used to generate the optimal water supply network configuration for five demand scenarios in the Zeeuws-Vlaanderen region for the years 2030, 2045, and 2110 (a total of 15 simulations). In each scenario the salinity of the water reaching the demand location differs while the demand volume is kept the same at 2.5 Mm^3 $year^{-1}$. The scenarios are:

1. The minimum possible salinity for water reaching the demand location
2. No salinity requirements for water reaching the demand location

After determining the salinity range in 1. and 2. three intermediate scenarios are simulated:

3. A salinity of 375 $mgCl^-$ L^{-1} or lower for water reaching the demand location
4. A salinity of 400 $mgCl^-$ L^{-1} or lower for water reaching the demand location

5. A salinity of 425 $mgCl^- L^{-1}$ or lower for water reaching the demand location

4.1 Network configurations for a minimum salinity at the demand location

The lowest possible salinity is determined by sorting well clusters in order of increasing salinity and by calculating the cumulative salinity based on the available water (see Supplementary Information 6). The set of the well clusters included in the WSN differs between 2030, 2045, and 2110 because the salinization/freshening rate is not equal for all well clusters. The minimum possible salinity for a demand of 2.5 Mm^{-3} $year^{-1}$ at the demand location is 246 $mgCl^- L^{-1}$ in 2030, 287 $mgCl^- L^{-1}$ in 2045, and 318 $mgCl^- L^{-1}$ in 2110.

Supplying water at the lowest possible salinity requires supply networks covering almost the complete study area (Figure 6). Such extensive networks are needed when high quality water is not available close to the demand site. The main difference between the 2030 simulation and the simulations of 2045 and 2110 is the use of well cluster 1. The salinity of well cluster 1 increases at a faster rate than other well clusters and is excluded from the minimum salinity network in favor of well cluster 16 in 2045 and 2110. Well cluster 21 also has a relatively high rate of salinization and is excluded in the 2110 network.

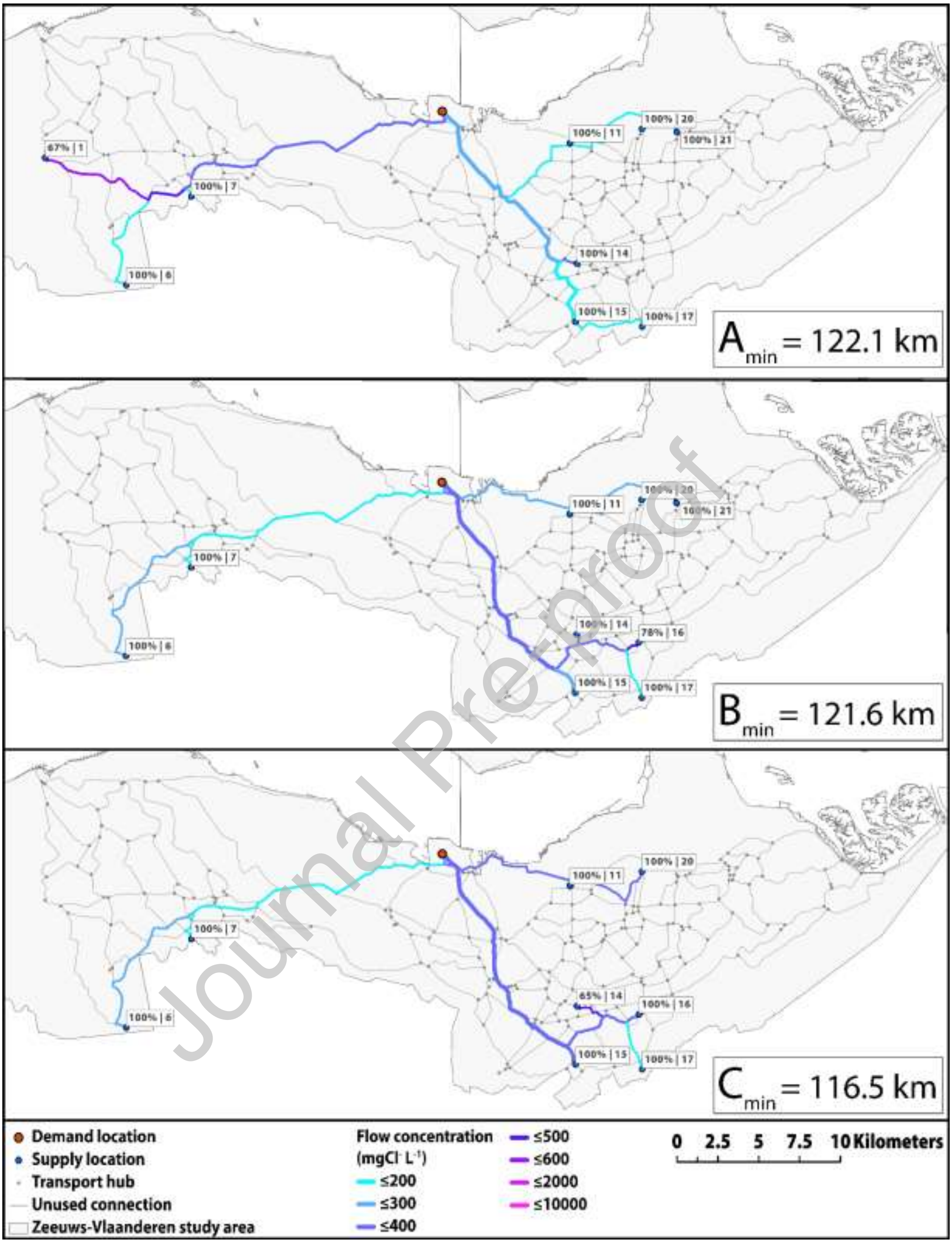

Figure 6 Optimal network configurations for the lowest possible salinity in 2030 (A_{min}, 246 mg Cl^- L^{-1}), 2045 (B_{min}, 287 mg Cl^- L^{-1}) and 2110 (C_{min}, 318 mg Cl^- L^{-1}). The well cluster labels show the rate (relative to water availability) at which the well clusters are operated and the well cluster number (operation rate | well cluster number).

433

4.2 Network configurations without salinity requirements at the demand location

Networks without a salinity requirement have an identical configuration, total length (46.9 km), and costs in 2030, 2045, and 2110 (Figure 7). The configuration is identical because the water quantity which can be extracted from each well cluster is considered constant. Due to salinization the resulting chloride concentrations at the demand location are 491 $mgCl^- L^{-1}$ in 2030, 510 $mgCl^- L^{-1}$ in 2045 and 529 $mgCl^- L^{-1}$ in 2110. The chloride concentration increase is 38 $mgCl^{-1}/L$ (±8%[2]) and is low compared to the overall 243 $mgCl^- L^{-1}$ (29%[3]) increase for the complete study area. The low salinization of the water supplied by the WSN is caused by freshening of well clusters 10,13, and 16.

The extraction rate from well cluster 14 is capped at 97% corresponding to a flow of 548 $m^3 day^{-1}$ with a pipeline diameter of 100 mm (see Table 2). Increasing the flow of this cluster would require a pipeline diameter of 200 mm, leading to higher costs. The amount of water that can be extracted from well cluster 10 is flexible and can be increased from 98% to 100% without increasing or decreasing the network investment costs. This flexibility can be used to provide slightly more water but leads to water with higher salinity at the demand location.

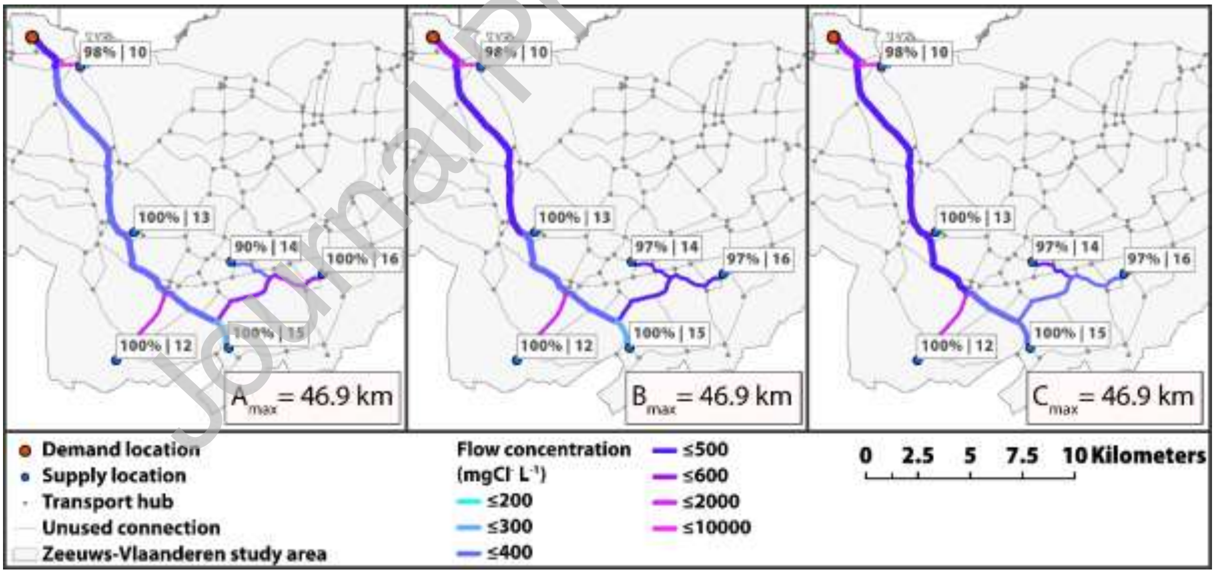

Figure 7 Optimal network configurations for networks without salinity requirements at the demand location in 2030 (A_{max}, 491 $mgCl^- L^{-1}$), 2045 (B_{max}, 510 $mgCl^- L^{-1}$) and 2110 (C_{max}, 529 $mgCl^- L^{-1}$). The well cluster labels show the rate (relative to water availability) at which the well clusters are operated and the cluster number (percentage | well cluster number).

2 (529 $mgCl^- L^{-1}$ - 491 $mgCl^- L^{-1}$) / 491 $mgCl^- L^{-1}$= 8%
3 (1095 $mgCl^- L^{-1}$ - 852 $mgCl^- L^{-1}$) / 852 $mgCl^- L^{-1}$= 29%, see last row of Supplementary Information 6

4.3 Network configurations for a salinity at the demand location of 375 $mgCl^- L^{-1}$, 400 $mgCl^- L^{-1}$, and 425 $mgCl^- L^{-1}$ or lower

The optimal network configurations for different periods and salinities at the demand site are shown in Figure 8. Small changes in demand quality (25 $mgCl^- L^{-1}$) affect the optimal configuration of the water supply network. The general trend is that the length, complexity, and costs of the supply network increase when groundwater with a lower salinity is required at the demand location. This trend is the most pronounced for the 2110 simulation; the optimal network for a demand quality of 425 $mgCl^- L^{-1}$ is 17.2 km shorter than for a demand of 375 $mgCl^- L^{-1}$ (see Figure 8 and Table 3). The salinization of well clusters leads to longer networks and increasing costs over time.

The networks A_2, A_3, and B_3 (see Figure 8) share the same configuration. This network configuration has a length of 51.8 km and is suitable between 2030 and 2045 for a salinity up to 425 $mgCl^- L^{-1}$. The difference with the network configuration without a salinity requirement at the demand location (section 4.2) is the addition of well cluster 17. Well cluster 17 is added because it provides enough fresh groundwater to reach the desired salinity.

The networks A_1, B_2, and C_3 (see Figure 8) also share the same configuration. This network configuration of 51.6 km is 0.1% more expensive than the 51.8 km network (A_2, A_3, and B_3). A shorter network can have higher costs depending on the specific pipeline diameters which need to be used. The salinity of the groundwater supplied by this network is lower than the required salinity of the demand site for any of the periods shown in Figure 8. For example, the chloride concentration of groundwater provided by network A_1 is 337 $mgCl^- L^{-1}$ instead of the maximum allowed concentration of 375 $mgCl^- L^{-1}$. This is possible due to the constraint in Eq. (10) which ensures that the salinity of groundwater reaching the demand location is lower than or equal to the demand salinity. A network which supplies groundwater with a lower salinity than the demand salinity, the case for A_1, B_2, and C_3, only occurs when the lowest cost network happens to yield a lower salinity.

The networks B_1, and C_2 (see Figure 8) share the same configuration. This network configuration has a length of 59.0 km and is needed for a demand salinity up to 375 $mgCl^{-1}$ by 2045. The C_1 network is created by connecting cluster 20 to the B_1/C_2 network resulting in a 68.8 km network.

For a detailed description of the characteristics of the network configurations see Supplementary Information 8 to Supplementary Information 10

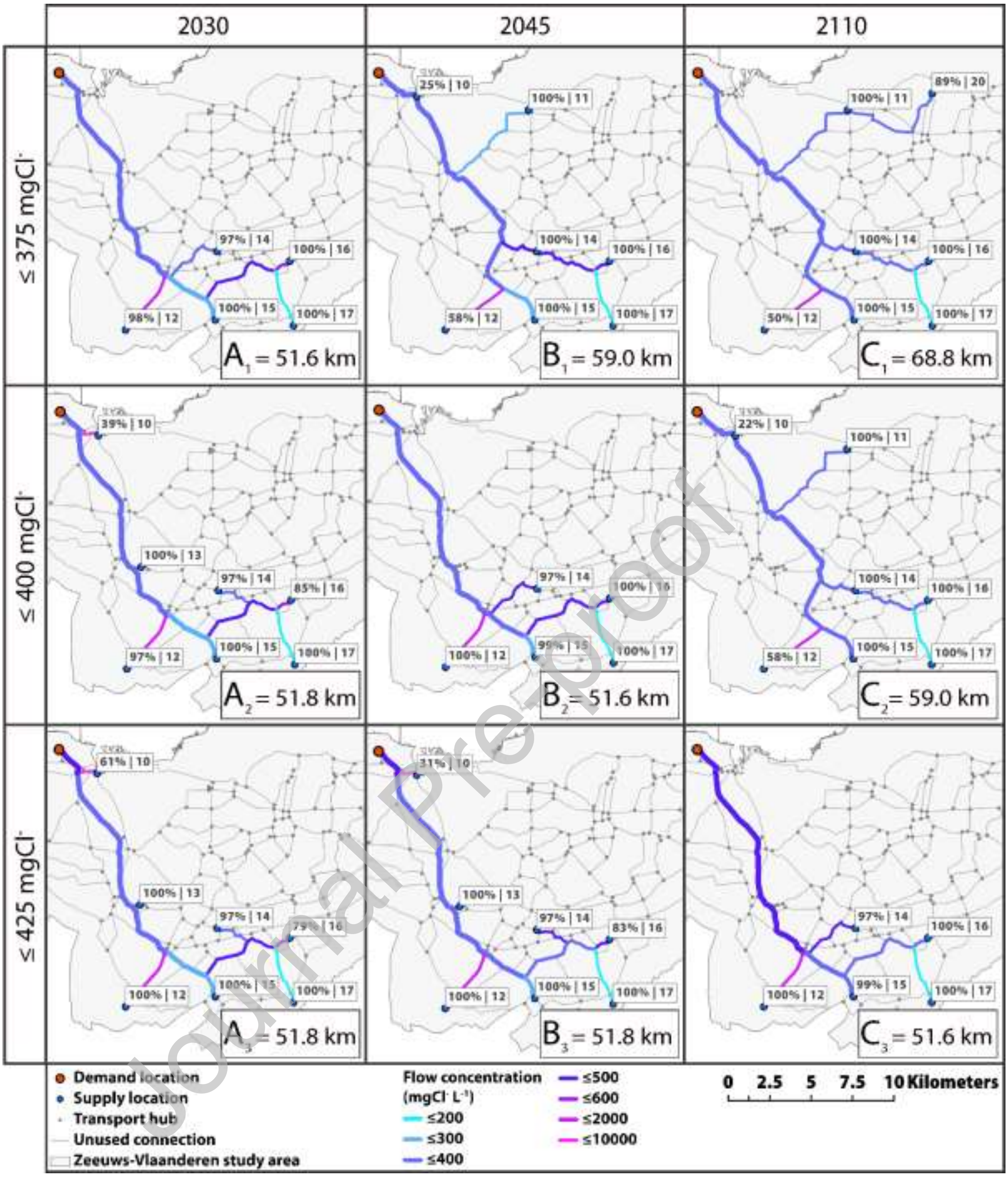

Figure 8 Optimal network configurations for the transport of water with a maximum salt concentration at the demand location of 375 mgCl$^-$ L^{-1}, 400 mgCl$^-$ L^{-1}, and 425 mgCl$^-$ L^{-1} in 2030, 2045 and 2110. The well cluster labels show the rate (relative to water availability) at which the well clusters are operated and the well cluster number (percentage | well cluster number).

4.4 Network costs in relation to salinity and time

As the maximum allowed salinity at the demand site increases, the length and costs of the WSN decrease (Table 3, from top to bottom). Increasing the maximum allowed salinity increases the number of well clusters which can be used in the network. A larger number of usable well clusters increases the probability that well clusters located close to the demand location can be used. The possibility to choose well clusters close to the demand location results in shorter networks. Shorter networks generally have lower costs, with some exceptions (see Section 4.3).

In general, the WSN costs increase when the same water quality needs to be supplied further in the future (Table 3, from left to right, except for the minimum salinity network). This is the result of the salinization of the well clusters in the study area. Salinization of well clusters results in fewer clusters which can contribute to the network for a specific demand salinity. As a result, longer networks which transport fresh water from further away are needed.

The optimal network configuration for a specific region depends on the local groundwater availability and the groundwater salinization/freshening dynamics. Salinization and freshening of specific well clusters can lead to unexpected WSN costs. For the Zeeuws-Vlaanderen simulation this is reflected in the optimal network configuration for the minimum possible salinity at the demand location when only using groundwater. Based on the modeled changes in groundwater salinity in Zeeuws-Vlaanderen the minimum salinity network for 2110 has lower costs compared to 2045 and 2030.

Table 3 Network length and costs. Costs are shown as a percentage in relation to the network without a salinity requirement at the demand site.

NETWORK	NETWORK LENGTH (km) | NETWORK COSTS[a]		
	2030	2045	2110
MINIMUM	122.1 | 168%	121.6 | 159%	116.5 | 153%
≤ 375 $mgCl^{-}$ L^{-1}	51.6[b] | 104%	59.0 | 107%	68.8 | 114%
≤ 400 $mgCl^{-}$ L^{-1}	51.8[b] | 104%	51.6 | 104%	59.0 | 107%
≤ 425 $mgCl^{-}$ L^{-1}	51.8 | 104%	51.8 | 104%	51.6 | 104%
NO SALINITY REQUIREMENT	46.9 | 100%	46.9 | 100%	46.9 | 100%

[a] Costs are normalized based on the scenario in which there is no salinity

requirement at the demand site

[b] Costs for the 51.6 km network are higher than the 51.8 km network due to the specific pipeline diameters needed

5 Discussion

5.1 WaterROUTE for regional planning

The modelling approach presented in this study expands the functionality of the WSN model (Willet et al., 2020) with the possibility to mix water and further expands the modelling toolbox on which Integrated Water Resources Management is reliant (Srdjevic et al., 2004). Determining the most cost-effective network for a specific quality at the demand site needs to consider different water qualities and water quantities at the supply sites. Input data on water quantity and water quality is supplied by existing and tested external hydrological models. WaterROUTE processes these inputs and makes it possible to explore water supply network options when the water quality of regional supply sources changes over time. It shows how small changes in the maximum allowed salinity of water reaching the demand location cause significant changes in the configuration of the water supply network. This knowledge is useful for regional planning purposes.

WaterROUTE can also be used to plan network expansion by using the characteristics of an existing supply network as inputs. For existing networks, the capacity of the existing pipelines is fixed but using these pipelines does not require new investments. Other characteristics of existing networks can also be incorporated. For example, if existing networks contain segments with iron pipelines a maximum salinity constraint for these pipeline sections can prevent corrosion when using saline/brackish water resources.

The possibility to include several demand locations, instead of a single demand location, for decentralized water supply network design and regional planning is relevant for areas where multiple water users compete for the same water resources. The addition of multiple demand locations, with different water demand quantities and qualities, introduces non-convex quadratic constraints to the optimization model and requires a problem formulation where several water flows of different qualities can flow over the same trajectory in parallel pipelines. Developing an effective problem formulation for multiple demand sites is suggested for future research.

5.2 Alternative water sources for industrial use

Decentralized supply networks making use of alternative water sources can be a solution to cope with future changes in water availability around the world. Decentralization of water supply can enhance water reuse possibilities (Leflaive, 2009) and can have advantages over centralized systems (Domènech, 2011; Leflaive, 2009; Piratla and Goverdhanam, 2015). Supplying industrial sites with alternative regional water resources requires data on the availability of alternative sources, now and in the future. WaterROUTE is a tool that can evaluate the feasibility of using these alternative sources and their corresponding decentralized supply networks at a high spatial resolution. Modeled brackish groundwater is used as the alternative water supply in the Zeeuws-Vlaanderen example simulation. Other alternatives, such as treated wastewater, rainwater, desalinated seawater, or surface water, can also be evaluated with WaterROUTE.

The formulation of the optimization problem in WaterROUTE is based on an overall mass balance of water and a product. The product used in the Zeeuws-Vlaanderen simulation is chloride. Other water quality parameters than chloride can also be used. Another possibility is to investigate multiple products simultaneously by adding new variables and constraints for each of the additional products to the basic model framework. This functionality is useful when evaluating other local alternative water sources such as rainwater and treated wastewater from industries, urban areas, and agriculture. When adding additional quality parameters non-linear and non-additive relationships between products should be accounted for. For example, two water steams originally free of microbial activity, the first due to a lack of nutrients, the second due to a lack of organic carbon, can lead to bacterial growth when mixed. The addition of these complex interactions is only possible when they can be accurately predicted mathematically but can lead to computational problems if relationships are non-linear. The fields of industrial ecology (Hond, 1999) and circular urban metabolism (Agudelo-Vera et al., 2012) can benefit from such additions for analysis and design. Within industrial ecology, specifically industrial symbiosis, providing water at a specific quality (fit for purpose) has been proposed to alleviate water shortages (Bauer et al., 2019).

5.3 Supply sources and sustainability

Groundwater extractions have inevitable consequences on local groundwater hydrology. Limiting the amount of groundwater extracted to renewable rates is one step towards sustainable exploitation of local water resources. WaterROUTE is suitable for designing water supply networks which respect sustainable extraction rates. This functionality is needed for regional planning that aims to anticipate on the expected changes in water availability (Hanasaki et al., 2013), salinization of (ground)water resources (H.D.

Holland and K.K. Turekian, 2003; UNEP, 2016), and the overall need to match resource utilization with the local/global carrying capacity (Bakshi et al., 2015). Within industrial water use the connection between local carrying capacity and evaluation methods for water use is still lacking (Willet et al., 2019). WaterROUTE provides a link between the physical (hydrological) modeling of water resources and regional planning of water supply networks. Through this link the costs for mismanagement of scarce water resources, e.g. overextraction leading to salinization requiring longer supply networks, becomes apparent.

In this study, the maximum groundwater extraction rates are made dependent on a maximum drawdown of the phreatic groundwater level for the complete region. It is proposed to replace regional values for maximum salinization and phreatic groundwater level drawdown by well cluster specific values in future research. Using well cluster specific values reveals the effect of sustainability thresholds at a higher spatial resolution on WSN design. Other possible criteria for groundwater extractions are the vulnerability of local ecosystems to salinization (Castillo et al., 2018; Herbert et al., 2015) and the susceptibility of soils to sodification (Minhas et al., 2019) (a nearly irreversible process).

The results of WaterROUTE show that in most scenarios not all well clusters are used, or well clusters are exploited below their maximum capacity. WaterROUTE does not yet consider the effects of partial extractions on the complete groundwater system. The simulations performed for this study suggest that interference between well clusters can be neglected for the Zeeuws-Vlaanderen area because well clusters are far enough apart. In other areas interference may occur and simulating the effects of partial extractions on groundwater salinity and drawdown to verify the feasibility of the network design is suggested. Simulating the effects of a network design on groundwater and subsequently updating the network design creates a dynamic interaction between the optimization model and the groundwater model. Such a dynamic interaction is relevant in areas where water extractions at one well cluster can affect other well clusters but is currently computationally infeasible.

The WaterROUTE model can also assist in designing regional water supply networks which counteract saltwater intrusion from the sea by using the WSN to recharge aquifers when fresh surface water is abundant. Smart groundwater extractions can lead to freshening of groundwater resources by attracting fresh water from the surface water systems instead of saline groundwater from below the extraction point. Coupling the operation of decentralized water supply networks with locations where this form of freshening is possible can lead to regional benefits besides water supply. Fresh water resources can be stored during the wet season to be retrieved at a later moment with Aquifer Storage and Recovery (ASR) (Maliva et al., 2006). Correct timing of extractions can make the stored water available for use without affecting the fresh-salt groundwater interface in the subsoil while being a cost effective option compared to other water supply alternatives (Oude Essink et al., 2018; Vink et al., 2010; Zuurbier et al., 2012). WaterROUTE is needed to design the supply network in which ASR sites are embedded.

5.4 Interactions with desalination

WaterROUTE can, in future work, be combined with desalination models to evaluate the potential for local supply networks in combination with (mild) desalination. Desalination of lower quality water provided by shorter and less expensive networks can be preferable over extensive networks which provide high quality water. The Zeeuws-Vlaanderen simulation shows that up to 2030 the 375 $mgCl^{-}$ L^{-1} network is not significantly more expensive than the 400 $mgCl^{-}$ L^{-1} or 425 $mgCl^{-}$ L^{-1} network. Supplying water at 375 $mgCl^{-}$ L^{-1} in 2110 leads to a significant increase in costs. Instead of expanding the supply network (mild) desalination can be applied to achieve the desired quality. Desalination technology improvements and optimization of treatment train design allow for treatment of a wide range of saline streams (McGovern et al., 2014). Several modeling approaches exist to design treatment trains optimized for a specific input stream (Skiborowski et al., 2012; Wreyford et al., 2020). Coupling a treatment train model which calculates the lowest treatment train costs, such as DESALT (Wreyford et al., 2020), with the costs for water transport can yield better overall system configurations. The performance of such systems can be evaluated through Multi-Criteria Decision Making techniques such as Data Envelopment Analysis (Belmondo Bianchi et al., 2020). Determining the optimal location for desalination systems (at the user, at the individual supply sites, or at mixing locations) within decentralized networks has implications for the energy system and is a next step within the water-energy nexus research field (Hussey and Pittock, 2012).

6 Conclusions

WaterROUTE is a valuable tool for planning and design of water supply networks using local alternative water sources. WaterROUTE designs water supply networks that deliver water at the specified quality and quantity of the user based on the modeled or known availability of water resources in a region. The model is used in an example simulation to show how the dynamics of groundwater resources can be connected to the regional design and planning of water supply networks. Long-term scenarios can be generated which help to anticipate on changes in (fresh)water availability. WaterROUTE is demonstrated with a simulation for Zeeuws-Vlaanderen, the Netherlands, and shows that a small decrease in demand quality (a chloride concentration increase from 375 $mgCl^{-}$ L^{-1} to 400 $mgCl^{-}$ L^{-1} in 2110) results in a decrease of the supply network placement costs by 7% for a demand of 2.5 Mm^{3} $year^{-1}$. Delivering higher quality water leads to higher costs because longer networks are needed. The length of the water supply network for the Zeeuws-Vlaanderen simulation varies between 46.9 km and 122.1 km based on the water quality required at the demand location. The WaterROUTE model shows that costs can be up to 68% higher to supply water with the lowest possible salinity compared to a demand with no salinity constraint in the Zeeuws-Vlaanderen simulation. The best network configuration depends on the specific water quality demand of the user, the local water availability, and the time horizon over which planning occurs. As water quality requirements become more stringent, optimal network selection becomes more complex and modeling tools such as WaterROUTE are needed to assist decision makers in designing cost-effective decentralized water supply networks. WaterROUTE can, in future work, be expanded, and can be used to determine the optimal balance between water transport and water treatment/desalination, the use of aquifer storage and recovery within decentralized networks, and the creation of decentralized water supply networks based on the exchange of water between urban, industrial, and agricultural areas. Through these applications WaterROUTE can assist in coping with regional water scarcity over time by connecting demand sites with local supply sources.

Declaration of competing interest

The authors confirm that there are no known conflicts of interest associated with this publication and there has been no significant financial support for this work that could have influenced its outcome.

CRediT authorship contribution statement

Joeri Willet: Project administration, Conceptualization, Methodology, Data curation, Visualization, Writing - original draft. **Koen Wetser**: Conceptualization, Supervision, Visualization, Writing - review & editing. **Jouke E. Dykstra**: Conceptualization, Supervision, Visualization, Writing - review & editing. **Alessio Belmondo Bianchi**: Conceptualization, Methodology, Writing – original draft. **Gualbert H.P. Oude Essink**: Methodology, Groundwater salinity modelling, Data generation and curation, Visualization, Writing – original draft. **Huub H.M. Rijnaarts**: Conceptualization, Funding acquisition, Supervision, Writing - review & editing.

Acknowledgements

This research is financed by the Netherlands Organisation for Scientific Research (NWO), which is partly funded by the Ministry of Economic Affairs and Climate Policy, and co-financed by the Netherlands Ministry of Infrastructure and Water Management and partners of the Dutch Water Nexus consortium. The regional partners: DOW Benelux, Evides, KWR, and Shell contributed to this project by providing the context for the example simulation, providing data on regional water demand, and practical expertise on the water supply system.

Competing interests statement

We wish to confirm that there are no known conflicts of interest associated with this publication and there has been no significant financial support for this work that could have influenced its outcome.

We confirm that the manuscript has been read and approved by all named authors and that there are no other persons who satisfied the criteria for authorship but are not listed. We further confirm that the order of authors listed in the manuscript has been approved by all of us.

We confirm that we have given due consideration to the protection of intellectual property associated with this work and that there are no impediments to publication, including the timing of publication, with respect to intellectual property. In so doing we confirm that we have followed the regulations of our institutions concerning intellectual property.

We understand that the Corresponding Author is the sole contact for the Editorial process (including Editorial Manager and direct communications with the office). He/she is responsible for communicating with the other authors about progress, submissions of revisions and final approval of proofs. We confirm that we have provided a current, correct email address which is accessible by the Corresponding Author

Signed by all authors as follows:

Joeri Willet (corresponding author), Koen Wetser, Jouke Dykstra, Alessio Belmondo Bianchi, Gualbert Oude Essink, Huub Rijnaarts

7 References

Actuel Hoogtebestand Nederland, 2020. AHN (accessed 25.05.2020). https://www.ahn.nl/.

Agudelo-Vera, C.M., Leduc, W.R.W.A., Mels, A.R., Rijnaarts, H.H.M., 2012. Harvesting urban resources towards more resilient cities. Resources, Conservation and Recycling 64, 3–12.

Atkinson, D.M., Deadman, P., Dudycha, D., Traynor, S., 2005. Multi-criteria evaluation and least cost path analysis for an arctic all-weather road. Applied Geography 25 (4), 287–307.

Awe, O.M., Okolie, S.T.A., Fayomi, O.S.I., 2019. Review of Water Distribution Systems Modelling and Performance Analysis Softwares. J. Phys.: Conf. Ser. 1378, 22067.

Bakshi, B.R., Ziv, G., Lepech, M.D., 2015. Techno-Ecological Synergy: A Framework for Sustainable Engineering. Environ. Sci. Technol. 49 (3), 1752–1760.

Bates, B.C., Kundzewicz Z.W., Wu S., Palutikof J.P., 2008. Climate Change and Water: Technical Paper of the Intergovernmental Panel on Climate Change. IPCC technical paper. IPCC Secretariat, Geneva, 210 pp.

Bauer, S., Behnisch, J., Dell, A., Gahr, A., Leinhos, M., Linke, H.J., Shen, W., Tolksdorf, J., Wagner, M., 2019. Water Reuse Fit for Purpose by a Sustainable Industrial Wastewater Management Concept. Chemie Ingenieur Technik 91 (10), 1472–1479.

Belmondo Bianchi, A., Wreyford, J.M., Willet, J., Gerdessen, J.C., Dykstra, J.E., Rijnaarts, H.H.M., 2020. Treatment vs. transport: A framework for assessing the trade-offs between on-site desalination and off-site water sourcing for an industrial case study. Journal of Cleaner Production, 124901.

Bornstein, C.T., Rust, R., 1988. Minimizing a sum of staircase functions under linear constraints. Optimization 19 (2), 181–190.

Bruggeman, G.A. (Ed.), 1999. Analytical Solutions of Geohydrological Problems. Developments in Water Science. Elsevier, Burlington.

Caldera, U., Breyer, C., 2017. Learning Curve for Seawater Reverse Osmosis Desalination Plants: Capital Cost Trend of the Past, Present, and Future. Water Resour. Res. 53 (12), 10523–10538.

Castillo, A.M., Sharpe, D.M.T., Ghalambor, C.K., León, L.F. de, 2018. Exploring the effects of salinization on trophic diversity in freshwater ecosystems: a quantitative review. Hydrobiologia 807 (1), 1–17.

Chee, R., Lansey, K., Chee, E., 2018. Estimation of Water Pipe Installation Construction Costs. J. Pipeline Syst. Eng. Pract. 9 (3), 4018008.

Clark, R., Cresswell, D., 2011. WaterCress User Manual.

Collischonn, W., Pilar, J.V., 2000. A direction dependent least-cost-path algorithm for roads and canals. International Journal of Geographical Information Science 14 (4), 397–406.

Dagan, G., Bear, J., 1968. Solving The Problem Of Local Interface Upconing In A Coastal Aquifer By The Method Of Small Perturbations. Journal of Hydraulic Research 6 (1), 15–44.

Delsman, J.R., Van Baaren, E.S., Siemon, B., Dabekaussen, W., Karaoulis, M.C., Pauw, P.S., Vermaas, T., Bootsma, H., Louw, P.G.B. de, Gunnink, J.L., Dubelaar, C.W., Menkovic, A., Steuer, A., Meyer, U., Revil, A., Oude Essink, G.H.P., 2018. Large-scale, probabilistic salinity mapping using airborne electromagnetics for groundwater management in Zeeland, the Netherlands. Environ. Res. Lett. 13 (8), 84011.

Doherty, J., 2005. PEST Model-Independent Parameter Estimation (User Manual). Watermark Numerical Computing.

Domènech, L., 2011. Rethinking water management: From centralised to decentralised water supplyand sanitation models. dag 57 (2), 293.

Douglas, D.H., 1994. Least-cost Path in GIS Using an Accumulated Cost Surface and Slopelines. Cartographica: The International Journal for Geographic Information and Geovisualization 31 (3), 37–51.

Du, D.Z., Pardalos, P.M. (Eds.), 1993. Network Optimization Problems: Algorithms, Applications and Complexity. Series on Applied Mathematics. WORLD SCIENTIFIC.

Faneca Sànchez, M., Gunnink, J.L., van Baaren, E.S., Oude Essink, G.H.P., Siemon, B., Auken, E., Elderhorst, W., Louw, P.G.B. de, 2012. Modelling climate change effects on a Dutch coastal groundwater system using airborne electromagnetic measurements. Hydrol. Earth Syst. Sci. 16 (12), 4499–4516.

Feldman, S.C., Pelletier, R.E., Walser, E., Smoot, J.C., Ahl, D., 1995. A Prototype for Pipeline Routing Using Remotely Sensed Data and Geographic Information System Analysis. Remote Sensing of Environment 53 (2), 123–131.

Gleick, P.H., 2003. Water Use. Annual Review of Environment and Resources 28 (1), 275–314.

H.D. Holland, K.K. Turekian (Eds.), 2003. Treatise on Geochemistry. Elsevier.

Haasnoot, M., Middelkoop, H., Offermans, A., van Beek, E., van Deursen, W.P.A., 2012. Exploring pathways for sustainable water management in river deltas in a changing environment. Climatic Change 115 (3-4), 795–819.

Hanasaki, N., Fujimori, S., Yamamoto, T., Yoshikawa, S., Masaki, Y., Hijioka, Y., Kainuma, M., Kanamori, Y., Masui, T., Takahashi, K., Kanae, S., 2013. A global water scarcity assessment under Shared Socio-economic Pathways – Part 2: Water availability and scarcity. Hydrol. Earth Syst. Sci. 17 (7), 2393–2413.

Herbert, E.R., Boon, P., Burgin, A.J., Neubauer, S.C., Franklin, R.B., Ardón, M., Hopfensperger, K.N., Lamers, L.P.M., Gell, P., 2015. A global perspective on wetland salinization: ecological consequences of a growing threat to freshwater wetlands. Ecosphere 6 (10), art206.

Hirsch, W.M., Dantzig, G.B., 1968. The fixed charge problem. Naval Research Logistics 15 (3), 413–424.

Hoekstra, A.Y., Mekonnen, M.M., 2012. The water footprint of humanity. Proceedings of the National Academy of Sciences of the United States of America 109 (9), 3232–3237.

Holmberg, K., 1994. Solving the staircase cost facility location problem with decomposition and piecewise linearization. European Journal of Operational Research 75 (1), 41–61.

Hond, F.d., 1999. Industrial ecology: a review. Regional Environmental Change 1 (2), 60–69.

Hussey, K., Pittock, J., 2012. The Energy–Water Nexus: Managing the Links between Energy and Water for a Sustainable Future. E&S 17 (1).

Kim, H.-J., Hooker, J.N., 2002. Solving Fixed-Charge Network Flow Problems with a Hybrid Optimization and Constraint Programming Approach. Annals of Operations Research 115 (1/4), 95–124.

Lange, W.J. de, Prinsen, G.F., Hoogewoud, J.C., Veldhuizen, A.A., Verkaik, J., Oude Essink, G.H.P., van Walsum, P.E.V., Delsman, J.R., Hunink, J.C., Massop, H.T.L., Kroon, T., 2014. An operational, multi-scale, multi-model system for consensus-based, integrated water management and policy analysis: The Netherlands Hydrological Instrument. Environmental Modelling & Software 59, 98–108.

Leflaive, X., 2009. Alternative Ways of Providing Water: Emerging Options and Their Policy Implications. OECD, 34 pp.

Mala-Jetmarova, H., Sultanova, N., Savic, D., 2017. Lost in optimisation of water distribution systems? A literature review of system operation. Environmental Modelling & Software 93, 209–254.

Maliva, R.G., Guo, W., Missimer, T.M., 2006. Aquifer storage and recovery: recent hydrogeological advances and system performance. Water environment research : a research publication of the Water Environment Federation 78 (13), 2428–2435.

McGovern, R.K., Zubair, S.M., Lienhard V, J.H., 2014. The benefits of hybridising electrodialysis with reverse osmosis. Journal of Membrane Science 469, 326–335.

Medema, W., McIntosh, B.S., Jeffrey, P.J., 2008. From Premise to Practice: a Critical Assessment of Integrated Water Resources Management and Adaptive Management Approaches in the Water Sector. E&S 13 (2).

Mekonnen, M.M., Hoekstra, A.Y., 2016. Four billion people facing severe water scarcity. Science advances 2 (2), e1500323.

Mesman, G.A.M., Meerkerk, M.A., 2009. Evaluatie ontwerprichtlijnen voor distributienetten. KWR, 48 pp. http://api.kwrwater.nl//uploads/2017/10/KWR-09.073-Evaluatie-ontwerprichtlijnen-voor-distributienetten-vertakte-netten.pdf.

Michael G. McDonald, Arlen W. Harbaugh, 1988. A modular three-dimensional finite-difference ground-water flow model: Techniques of Water-Resources Investigations 06-A1. U.S. Geological Survey., 586 p.

Minhas, P.S., Qadir, M., Yadav, R.K., 2019. Groundwater irrigation induced soil sodification and response options. Agricultural Water Management 215, 74–85.

Oude Essink, G.H.P., 2001. Salt Water Intrusion in a Three-dimensional Groundwater System in The Netherlands : A Numerical Study. Transport in Porous Media 43 (1), 137–158.

Oude Essink, G.H.P., Pauw, P.S., van Baaren, E.S., Zuurbier, K.G., Louw, P.G.B. de, Veraart, J.A., MacAteer, E., van der Schoot, M., Groot, N., Cappon, H., Waterloo, M.J., Hu-A-Ng, K.R.M., Groen, M.A., 2018. GO-FRESH: Valorisatie kansrijke oplossingenvoor een robuuste zoetwatervoorziening: Rendabel en duurzaam watergebruik in een zilte omgeving.

Oude Essink, G.H.P., van Baaren, E.S., Louw, P.G.B. de, 2010. Effects of climate change on coastal groundwater systems: A modeling study in the Netherlands. Water Resour. Res. 46 (10).

Piratla, K.R., Goverdhanam, S., 2015. Decentralized Water Systems for Sustainable and Reliable Supply. Procedia Engineering 118, 720–726.

Plappally, A.K., Lienhard, J.H., 2013. Costs for water supply, treatment, end-use and reclamation. Desalination and Water Treatment 51 (1-3), 200–232.

Post, V., Kooi, H., Simmons, C., 2007. Using hydraulic head measurements in variable-density ground water flow analyses. Ground water 45 (6), 664–671.

Reddy, K.V., Ghaffour, N., 2007. Overview of the cost of desalinated water and costing methodologies. Desalination 205 (1-3), 340–353.

Savenije, H.H.G., van der Zaag, P., 2008. Integrated water resources management: Concepts and issues. Physics and Chemistry of the Earth, Parts A/B/C 33 (5), 290–297.

Shiklomanov, I.A., 1998. World water resources: a new appraisal and assessment for the 21st century. Unesco, 40 pp.

Sieber, J., Purkey, D., 2015. WEAP: Water Evaluation and Planning System User Guide.

Skiborowski, M., Mhamdi, A., Kraemer, K., Marquardt, W., 2012. Model-based structural optimization of seawater desalination plants. Desalination 292, 30–44.

Sonaje, N., Joshi, M., 2015. A REVIEW OF MODELING AND APPLICATION OF WATER DISTRIBUTION NETWORKS (WDN) SOFTWARES. International Journal of Technical Research and Applications e-ISSN: 2320-8163 3, 174–178.

Srdjevic, B., Medeiros, Y.D.P., Faria, A.S., 2004. An Objective Multi-Criteria Evaluation of Water Management Scenarios. Water Resources Management 18 (1), 35–54.

Stafleu, J., Maljers, D., Gunnink, J.L., Menkovic, A., Busschers, F.S., 2011. 3D modelling of the shallow subsurface of Zeeland, the Netherlands. Netherlands Journal of Geosciences 90 (4), 293–310.

UN Water - FAO, 2007. Coping with water scarcity - Challenge of the twenty-first century. UN Water - FAO, 29 pp.

UNEP, 2016. A Snapshot of the World’s Water Quality: Towards a global assessment. United Nations Environment Programme, Nairobi, Kenya., 162 pp.

United Nations, Department of Economic and Social Affairs, Population Division, 2019. World Population Prospects 2019 Highlights (ST/ESA/SER.A/423), 46 pp.

Van Baaren, E.S., Oude Essink, G.H.P., Janssen, G.M.C.M., Louw, P.G.B. de, Heerdink, R., Goes, B., 2016. Verzoeting en verzilting van het grondwater in de Provincie Zeeland, Regionaal 3D model voor zoet-zout grondwater, Deltares rapport 1220185, 86 pp. https://publicwiki.deltares.nl/download/attachments/55640066/1220185-000-BGS-0003-r-Verzoeting%20en%20verzilting%20freatisch%20grondwater%20in%20de%20Provincie%20Zeeland-def.pdf?version=1&modificationDate=1490345125944&api=v2 (accessed 27.05.2021).

Vink, K., Rambags, F., Gorski, N., 2010. Freshmaker: Technologie voor een duurzame zoetwatervoorziening. Freshmaker: Technology for sustainable fresh water supply. KWR.

Vörösmarty, C.J., Green, P., Salisbury, J., Lammers, R.B., 2000. Global water resources: vulnerability from climate change and population growth. Science 289 (5477), 284–288.

Willet, J., King, J., Wetser, K., Dykstra, J.E., Oude Essink, G.H.P., Rijnaarts, H.H.M., 2020. Water supply network model for sustainable industrial resource use a case study of Zeeuws-Vlaanderen in the Netherlands. Water Resources and Industry 24, 100131.

Willet, J., Wetser, K., Vreeburg, J., Rijnaarts, H.H.M., 2019. Review of methods to assess sustainability of industrial water use. Water Resources and Industry 21, 100110.

Wreyford, J.M., Dykstra, J.E., Wetser, K., Bruning, H., Rijnaarts, H.H.M., 2020. Modelling framework for desalination treatment train comparison applied to brackish water sources. Desalination 494, 114632.

Zhou, J., Peng, J., Liang, G., Deng, T., 2019. Layout optimization of tree-tree gas pipeline network. Journal of Petroleum Science and Engineering 173, 666–680.

Zuurbier, K.G., Paalman, M., Zwinkels, E., 2012. Haalbaarheid Ondergrondse Waterberging Glastuinbouw Westland. Feasibility of Aquifer Storage and. KWR Watercycle Research Institute, Nieuwegein.

8 Supplementary Information

Supplementary Information 1 Pipeline placement costs based on flow requirements and a cost of 0.5 € mm^{-1} diameter m^{-1}. Each plateau represents an available pipeline diameter, starting at 100mm with increments of 100mm, in which the flow velocity is within the optimal range (0.5 m s^{-1}

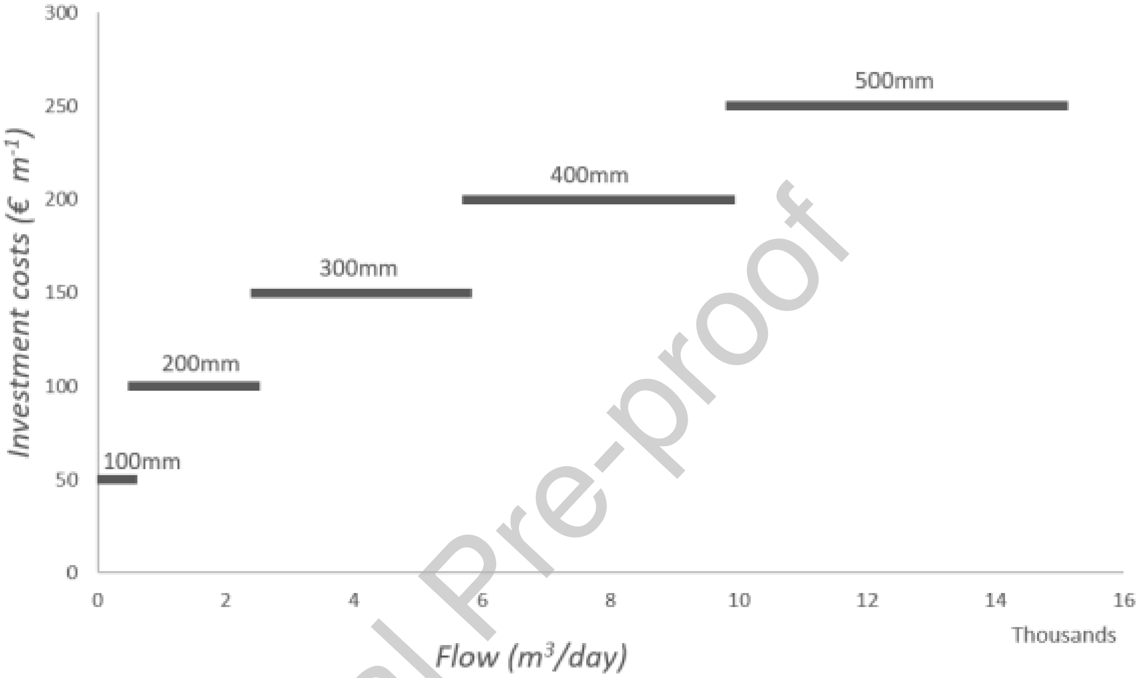

and 1.5 m s^{-1}).

Supplementary Information 2 Procedure for well placement and drawdown determination

Methodology to determine the extraction and drawdown of well clusters in Zeeuws-Vlaanderen

The distribution of well clusters over the Zeeuws-Vlaanderen region and number of extraction wells was one-to-one adopted from Willet et al. (2020). We use a 100 m spaced well cluster grid as the model has also a spatial model cell distribution of 100m.

The choice was made to optimize the extractions, rather than optimizing the well placement based on extraction possibilities, since the extraction wells will likely affect each other within a well cluster. In an iterative process the extraction rate per extraction well is adapted until the maximum drawdown of the phreatic groundwater level in a well cluster is at maximum 50 mm. The procedure is as follows:

1. The model starts with rates at each extraction well that are retrieved from Willet et al. (2020).
2. The model is run for one year to determine a steady-state piezometric head distribution.
3. The drawdown of the phreatic groundwater level at each well cluster due to the extraction well scheme is assessed by comparing the piezometric head distribution with a model without extraction wells. If the drawdown at an extraction well is more than 50 mm, the extraction rate is reduced; if it is less, the extraction rate is increased. This fraction is equal to 0.05/(piezometric head without extraction wells minus piezometric head with extraction wells).
4. The model is run again, and the procedure is repeated for in total ninety-nine times. In general, after thirty iterations the total groundwater extraction rate does not change significantly anymore (and differs less than 0.1% from the value after ninety-nine iterations).

This procedure yields an approximation for the optimized extraction scheme over the extraction wells per well clusters over the entire region. In this approach, we neglect the effect that the groundwater salinity change has on piezometric heads; this is acceptable as we are dealing with only fresh to light brackish groundwater in the extraction wells.

5. The model is run again with the optimized extraction well scheme for the period 2020-2110 to determine the change of the chloride concentration over time. Every 10 days, the average chloride concentration that belongs to each well in each well cluster is determined (we account for the rate per well as they differ). In most wells, the average chloride concentration increases due to upconing, but the increase is small as the extraction rate per well is quite modest (the maximum drawdown is only 50mm).

Reference: Willet, J., King, J., Wetser, K., Dykstra, J.E., Oude Essink, G.H.P., Rijnaarts, H.H.M., 2020. Water supply network model for sustainable industrial resource use a case study of Zeeuws-Vlaanderen in the Netherlands. Water Resources and Industry 24, 100131.

860 *Supplementary Information 3 Procedure to generate minimum salinity networks*

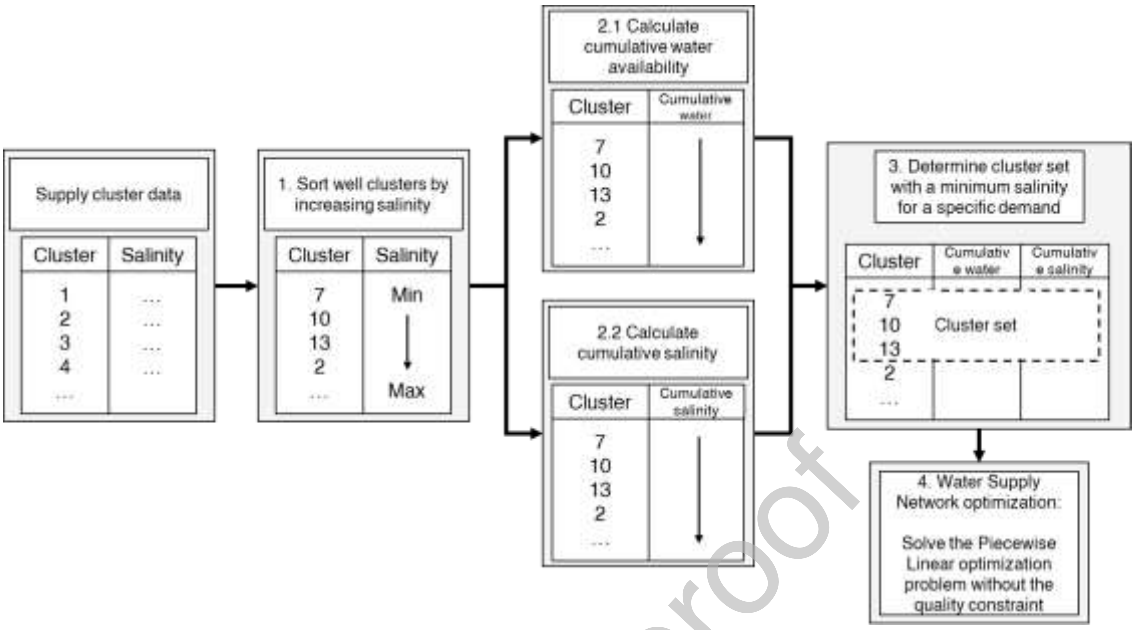

1. The well cluster data is sorted by increasing salinity in step 1.
2. In step 2.1 and 2.2 the cumulative water availability and salinity are determined.
3. The cumulative water available at cluster 2 in the figure is given by the sum of water from well clusters 7, 10, 13, and 2.
4. The cumulative salinity is determined by the sum of the total amount of salt from each well cluster divided by the total amount of water.

5. Based on the water demand at the demand site the minimum possible salinity can be determined by looking up the volume in the combined table from 2.1 and 2.2. This yields the cluster set which can provide the minimum possible salinity for that level of demand. This cluster set is used for the optimization procedure.

6. The optimization model is used to determine the optimal network layout. The quality constraints are disabled because the amount of water coming from each cluster has already been determined.

Journal Pre-proof

Supplementary Information 4 Water extraction rate and average chloride concentration per cluster in 2020, 2030, 2045 and 2110.

CLUSTER	EXTRACTION RATE (Mm^3 $year^{-1}$)	SALINITY ($mgCl^-$ L^{-1})			
		2020	**2030**	**2045**	**2110**
1	0.508	2	519	637	747
2	0.010	9243	9828	10164	10353
3	0.046	212	1454	1825	2195
4	0.079	684	1761	2518	3134
5	0.315	0	553	756	926
6	0.107	75	173	201	213
7	0.130	1	82	118	153
8	0.498	174	922	1171	1351
9	0.088	188	1223	1391	1543
10	0.059	7464	5449	4641	4052
11	0.117	78	187	287	375
12	0.343	196	638	786	923
13	0.046	2518	1523	1424	1365
14	0.206	263	394	411	402
15	1.432	8	210	266	325
16	0.436	1327	570	486	382
17	0.099	0	23	38	57
18	0.060	415	899	1002	1087
19	0.154	1068	1193	1068	968
20	0.046	0	7	98	382
21	0.024	0	175	410	668
22	0.220	818	1593	1779	1934

23	0.757	414	1247	1469	1630
24	0.086	2331	3186	3181	3147
25	0.253	1816	3160	3863	4602
TOTAL	6.119	472	852	981	1095

Supplementary Information 5 Simulated well clusters concentrations from 2020-2110. Each line represents one well cluster.

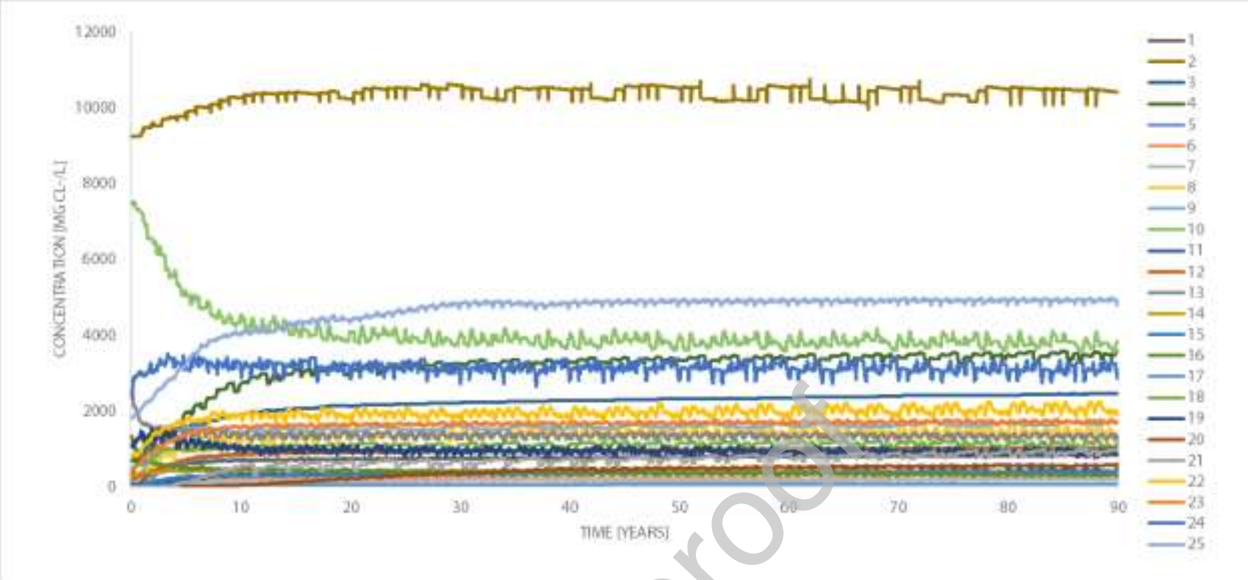

866

Supplementary Information 6 Cumulative water salinity (mgCl^- L^{-1}) and cumulative water availability (Mm^{-3} $year^{-1}$). The dark shaded rows indicate that covering a demand of 2.5 Mm^{-3} $year^{-1}$ requires water up to and including the shaded cluster.

2030			**2045**			**2110**		
Cluster	Salinity	Water	Cluster	Salinity	Water	Cluster	Salinity	Water
20	6	0.05	17	38	0.10	17	57	0.10
17	17	0.15	20	57	0.15	7	112	0.23
7	48	0.28	7	86	0.28	6	144	0.34
6	83	0.38	6	118	0.38	15	290	1.77
21	88	0.41	15	235	1.81	11	296	1.89
11	110	0.52	11	238	1.93	20	298	1.93
15	184	1.96	21	240	1.96	16	313	2.37
14	204	2.16	14	256	2.16	14	320	2.57
1	264	2.67	16	295	2.60	21	324	2.60
5	294	2.98	1	351	3.11	1	393	3.11
16	329	3.42	5	388	3.42	12	446	3.45
12	357	3.76	12	424	3.76	5	486	3.76
18	366	3.82	18	433	3.82	19	505	3.92
8	430	4.32	19	458	3.98	18	514	3.98
19	456	4.48	8	537	4.48	8	607	4.48
9	471	4.56	9	554	4.56	13	614	4.52
23	581	5.32	13	562	4.61	9	632	4.61
3	589	5.37	23	690	5.37	23	773	5.37
13	597	5.41	22	733	5.59	22	819	5.59
22	636	5.63	3	742	5.63	3	830	5.63
4	651	5.71	4	767	5.71	4	862	5.71
25	758	5.96	24	802	5.80	24	896	5.80
24	792	6.05	25	930	6.05	10	928	5.86
10	837	6.11	10	966	6.11	25	1080	6.11
2	852	6.12	2	981	6.12	2	1095	6.12

Supplementary Information 7 Preliminary network over which flows are optimized. The network was generated using least cost path methods as described in: Willet, J., Wetser, K., Vreeburg, J., Rijnaarts, H.H.M., 2019. Review of methods to assess sustainability of industrial water use. Water Resources and Industry 21, 100110.

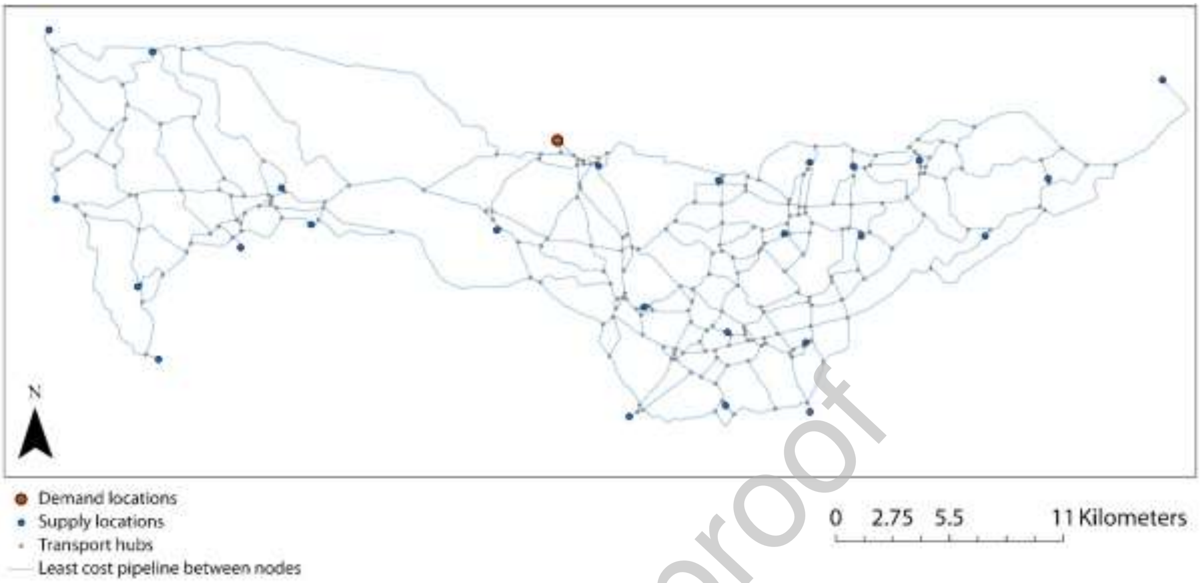

872

Supplementary Information 8 Network configurations for a salinity at the demand location of 375 mgCl^{-} L^{-1} *or lower*

The optimal networks for a maximum salinity of 375 $mgCl^- L^{-1}$ vary significantly between 2030, 2045, and 2110 (Figure). This is reflected in the length of the required network which increases from 51.6 km to 68.8 km (Table), an increase of 33%, from 2030 to 2110. The main difference between the scenarios is the addition/exclusion of well clusters and the configuration to connect well clusters 14, 16 and 17 to the rest of the network. The differences in the networks in chronological order are:

- 2030 (Figure 1, A_1) to 2045 (Figure 1, B_1): well clusters 10 and 11 are added to the network. Well cluster 11 is needed for its low salinity. Well cluster 10 has a high salinity, 4641 $mgCl^- L^{-1}$, but is added to the network to ensure the demand is covered. Adding well cluster 10 to the network makes it possible to reduce the flow from cluster 12 to 548 m^3 day^{-1}, which reduces the required pipeline diameter from cluster 12 to junction 12|15. Cluster 14 needs to be operated at 100% instead of 97%, requiring an increase in pipeline diameter. The addition of cluster 11 to the network moves the main branch of the network to the east.
- 2045 (Figure 1, B_1) to 2110 (Figure 1, C_1): salinization of the well cluster requires expansion of the network. Cluster 20 is added to the network to reach the desired water quality, and well cluster 10 is excluded. The operation capacity of cluster 12 is further reduced from 58% to 50%. This reduction is purely needed to reach the desired water quality at the demand location.

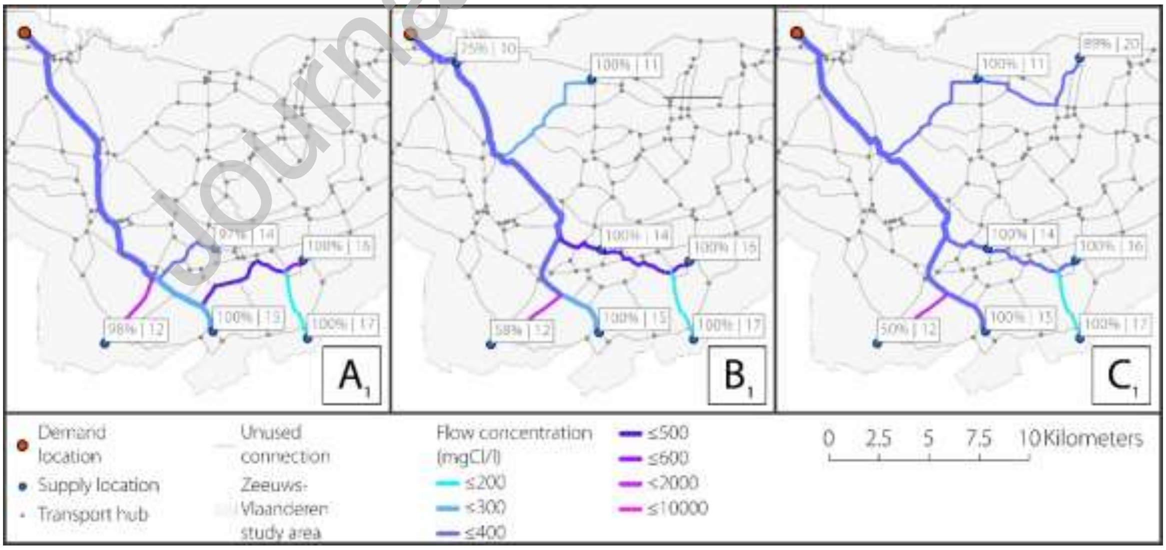

Figure 1 Optimal network configurations for a maximum of 375 $mgCl^- L^{-1}$ in 2030 (A, 337 $mgCl^- L^{-1}$), 2045 (B, 375 $mgCl^- L^{-1}$) and 2110 (C, 375 $mgCl^- L^{-1}$). The labels show the rate (relative to water availability) at which the well clusters are operated and the cluster number (percentage | cluster number)

The water supplied by the 2030 network reaches the demand location with a concentration of 337 mgCl⁻ L⁻¹ instead of 375 mgCl⁻ L⁻¹ (Table). This indicates that a network with lower costs than a network which provides 375 mgCl⁻ L⁻¹ exists. The specific combination of water availability and water quality at each cluster at this specific point in time makes this possible. The difference in quality over time is highest for the 2030 network (73 mgCl⁻ L⁻¹) and lowest for the 2045 network (58 mgCl⁻ L⁻¹).

Table 1 Cost and salinity effects of using 375 mgCl⁻ L⁻¹ networks at different periods

375 mgCl⁻¹ L⁻¹ NETWORK (NETWORK | COSTS | LENGTH)	**APPLIED IN 2030** (mgCl⁻ L⁻¹)	**APPLIED IN 2045** (mgCl⁻ L⁻¹)	**APPLIED IN 2110** (mgCl⁻ L⁻¹)
A_1 | 100% |51.6 km	337	376	410
B_1 | 103% | 59.0 km	344	375	402
C_1 | 110% | 68.8 km	306	341	375

Supplementary Information 9 Network configurations for a salinity at the demand location of 400 mgCl⁻ L^{-1} or lower

Networks for a maximum salinity at the demand location of 400 $mgCl^{-} L^{-1}$ have similar costs and configurations for 2030 and 2045. Achieving the same salinity in 2110 requires a different network configuration (Figure 2). The length of the networks reduces from 51.8 km in 2030 to 51.6 km in 2045 and increases to 59.0 km in 2110. The differences in the networks in chronological order are:

- 2030 (Figure 2, A_2) to 2045 (Figure 2, B_2): well clusters 10 and 13 can be removed from the network by increasing the capacity at which cluster 16 is operated from 85% to 100%. Cluster 16 is crucial for the network because salinity significantly decreases over time. Cluster 14 is connected to the rest of the network by going west (2045) instead of east (2030). This change is needed to avoid increasing the pipeline capacity at the junction of cluster 15 with clusters 14|16|17.
- 2045 (Figure 2, B_2) to 2110 (Figure 2, C_2): cluster 10 and 11 are added to the network. Cluster 14 is operated at 100% instead of 97% which changes the configuration of the network. Cluster 12 is operated at 58% to reduce the required pipeline diameter and cluster 10 is used to provide the remaining water.

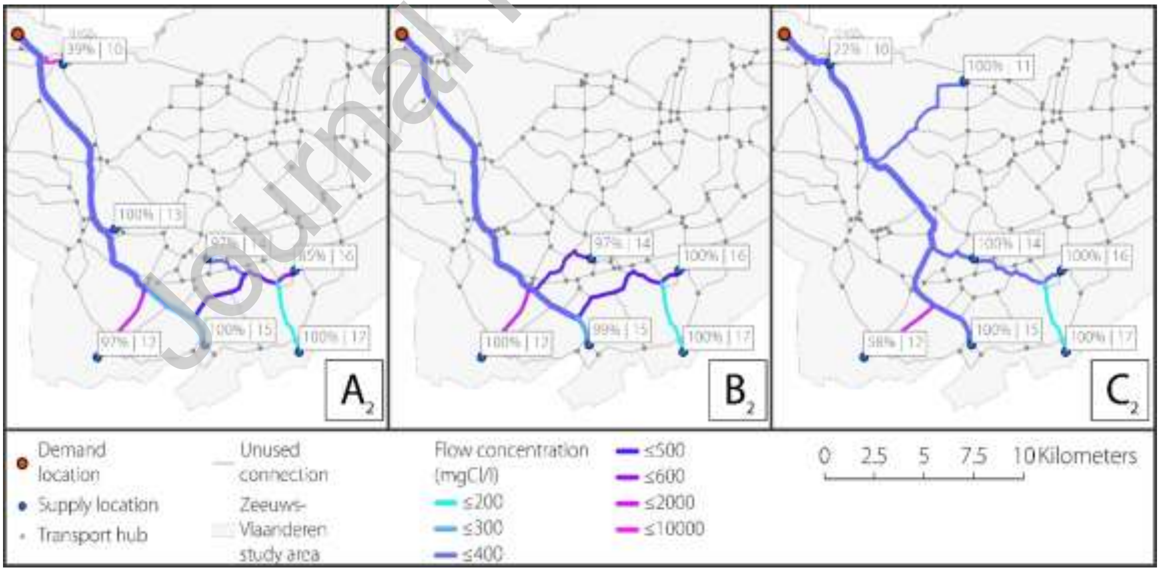

Figure 2 Optimal network configurations for a maximum of 400 $mgCl^{-} L^{-1}$ in 2030 (A, 400 $mgCl^{-} L^{-1}$), 2045 (B, 378 $mgCl^{-} L^{-1}$) and 2110 (C, 400 $mgCl^{-} L^{-1}$). The labels show the rate (relative to water availability) at which the well clusters are operated and the cluster number (percentage | cluster number)

The 2110 network supplies water with the smallest difference in salinity over time (59 $mgCl^{-} L^{-1}$, Table

2). The 2045 network supplies water with a concentration of 378 $mgCl^{-} L^{-1}$ instead of 400 $mgCl^{-} L^{-1}$. Flexibility off all networks is limited by the maximum capacity of the pipelines in combination with water availability at the supply sites. For the 2030 network increasing the water supplied by clusters 14 or 16 requires increasing pipeline capacity, while increasing extractions from clusters 10 or 12 has a high impact on water quality. The 2045 network operates most clusters at, or close to, maximum capacity. The 2110 network operates all low salinity clusters at 100% capacity.

Table 2 Cost and salinity effects of using 400 $mgCl^{-} L^{-1}$ networks at different periods

400 $mgCl^{-1} L^{-1}$ NETWORK (NETWORK | COSTS | LENGTH)	APPLIED IN 2030 ($mgCl^{-} L^{-1}$)	APPLIED IN 2045 ($mgCl^{-} L^{-1}$)	APPLIED IN 2110 ($mgCl^{-} L^{-1}$)
A_2 | 100% | 51.8 km	400	432	462
B_2 | 100% | 58.1 km	339	378	412
C_2 | 104% | 59.0 km	341	372	400

Supplementary Information 10 Network configurations for a salinity at the demand location of 425 $mgCl^{-} L^{-1}$ or lower

The networks for 425 $mgCl^{-} L^{-1}$ are the same in 2030 and 2045 but changes for 2110 (Figure 3). The networks for 425 $mgCl^{-} L^{-1}$ practically have the same costs (Figure 3). Freshening of cluster 16 makes it possible to reach the desired water quality over time while keeping costs at the same level. In 2110 clusters 10 and 13 are removed from the network because cluster 16 is operated at a higher capacity. The differences in the networks in chronological order are:

- 2030 (Figure 3, A_3) to 2045 (Figure 3, B_3): The network configuration remains the same. Cluster 16 is operated at a higher capacity to reach the desired salinity while cluster 10 is operated at a lower capacity.
- 2045 (Figure 3, B_3) to 2110 (Figure 3, C_3): cluster 10 and 13 are removed from the network. Cluster 16 is operated at 100% capacity instead of 86%. Cluster 14 connects to the main branch going west instead of east. This configuration change is needed to avoid increasing pipeline capacity at the junction of cluster 15.

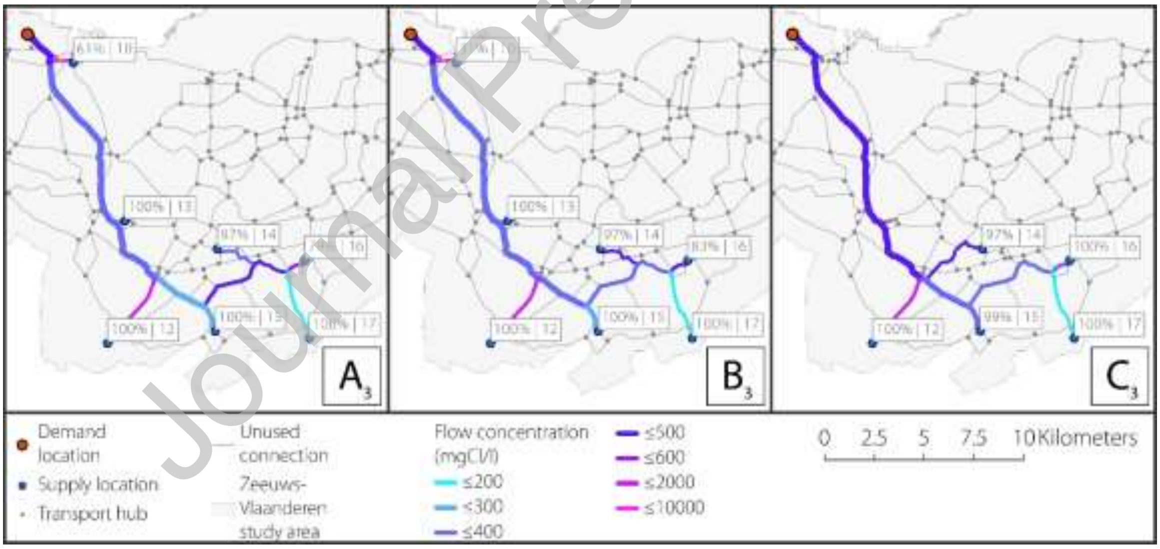

Figure 3 Optimal network configurations for a maximum of 400 $mgCl^{-} L^{-1}$ in 2030 (A, 400 $mgCl^{-} L^{-1}$), 2045 (B, 378 $mgCl^{-} L^{-1}$) and 2110 (C, 400 $mgCl^{-} L^{-1}$). The labels show the rate (relative to water availability) at which the well clusters are operated and the cluster number (percentage | cluster number)

The 2030 network has the smallest difference in water quality when applied in a different period (58 $mgCl^{-} L^{-1}$). The 2110 network supplies water at 412 $mgCl^{-} L^{-1}$ instead of 425 $mgCl^{-} L^{-1}$ because this leads to a lower cost network (). The 2110 network is the most efficient because all clusters are operated close to or at maximum capacity (cluster 15 can provide 1% more water, cluster 14 cannot provide more water without increasing pipeline capacity).

Table 3 Cost and salinity effects of using 425 $mgCl^{-}$ L^{-1} networks at different time periods

425 $mgCl^{-1}$ L^{-1} NETWORK (NETWORK | COSTS | LENGTH)	**APPLIED IN 2030** ($mgCl^{-}$ L^{-1})	**APPLIED IN 2045** ($mgCl^{-}$ L^{-1})	**APPLIED IN 2110** ($mgCl^{-}$ L^{-1})
A_3 | 100% | 51.8 km	425	454	483
B_3 | 100% | 51.8 km	391	425	457
C_3 | 100% | 51.6 km	339	378	412